SEISMIC ACADEMY

Seismic
A C A D E M Y
JOURNAL

EARTHQUAKES

- Articles
- Events
- Seismic Splendour

SEISMIC ACADEMY

A forum for professionals, academicians, authorities and industry experts to interact and disseminate knowledge on various aspects of earthquake engineering with different stakeholders, with an intent to increase awareness and develop their expertise on the subject.

OUR VISION

To make seismic academy as one source of information and use it for promotion of all seismic initiatives in our country.

OUR ADVISORY BOARD

A **CE&CR** PRODUCTION

IN THIS ISSUE - Total No. of Pages: 40 (Including Cover)

For further information, contact -
Shounak Mitra, Head - Codes & Approvals (Fastening), Hilti India Pvt. Ltd.
M: 9899732127 | E: support@theseismicacademy.com

TABLE OF
CONTENTS

ANNUAL CONFERENCE 2024
4TH SEPTEMBER '24, NEW DELHI

Hilti India Pvt. Ltd. launched the **Seismic Academy** as a forum for professionals, academics, authorities, and industry experts to connect and share knowledge on various seismic issues related to earthquake engineering. The initiative aims to raise awareness and enhance expertise among different stakeholders. With a vision to become one source of information for all earthquake related topics in India, the Seismic Academy has evolved, since its inception, through different initiatives.

On 4th September '24, the Academy held its Third Annual Conference at the India Habitat Center, Delhi, focusing on "**The Seismic Shift**" event brought together industry professionals, practicing consultants, renowned academicians and research scholars, along with distinguished experts from prominent government bodies for a full day of knowledge exchange on cutting-edge research, practical applications, and innovations in seismic engineering.

The conference started with a welcome address by Er. Jayant Kumar, Managing Director, Hilti India Pvt. Ltd., who provided a summary of the Seismic Academy's ongoing efforts and underscored the importance of fostering collaboration to strengthen seismic awareness and preparedness across sectors.

The highlight of the morning session was a keynote lecture by Mr. Anurag Sinha, Executive Director, Engineers India Ltd., a prominent figure in the field of seismic engineering, who delivered an in-depth presentation on emerging trends in seismic engineering with a focus on Early Data Warning System and its implementation in India .

The keynote session was followed by technical sessions. The first among them was delivered by Dr. Naveet Kaur, Senior Scientist, Bridge Engineering & Structures, CSIR - Central Road Research Institute, on the use of Unmanned Aerial Vehicles (UAVs) for the condition assessment of structures. Her talk shed light on how UAVs are revolutionizing the way we inspect and monitor the health of buildings, particularly in post-seismic scenarios, where timely assessments are critical.

Next, Dr. Ashwin Kumar P.C., Assistant Professor, Earthquake Engineering Department, Indian Institute of Technology (IIT) Roorkee shared his advanced research on enhancing seismic performance of structures. His detailed analysis explored modern techniques and materials that significantly improve the resilience of buildings, offering attendees a glimpse into the future of seismic-proof construction methods.

Mr. Hariharan Iyer, Director - B+P India, West Region Operational Lead, Structural Engineering Practice Lead - India delivered an insightful session on key seismic considerations, emphasizing on the revision of seismic standards in India and also offering a practical approach for engineers and architects designing in seismically active regions. His session was followed by two compelling case studies on structural retrofitting.

Dr. Mangesh Joshi, Managing Director & CEO, Sanrachana Structural Strengthening Pvt. Ltd., presented an in-depth case study on structural retrofitting techniques, focusing on real-world applications and lessons learned from retrofitting complex structures.

Dr. Jayanta Pathak, Head of Department, Assam Engineering College and Mr. Shounak Mitra, Head of Codes & Approval, Hilti India showcased a fascinating case study on hospital retrofit projects, highlighting the challenges and solutions implemented to ensure critical healthcare infrastructure can withstand seismic events without compromising patient care.
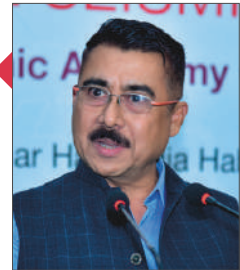
The technical sessions were chaired by the likes of who made it possible to have great exchange of ideas and knowhow corresponding to each topic.

The Seismic Shift Annual Conference 2024 provided a unique opportunity for attendees to not only learn about the latest seismic technologies and methodologies but also engage in discussions that will shape the future of seismic resilience in India. With a growing focus on safeguarding infrastructure, particularly in high-risk areas, this conference was a key step toward fostering a collaborative approach to mitigating seismic risks.

The event was Managed by Revered Media, a unit of CE&CR.

Felicitating the Session Chairs

THE PETRONAS TOWERS

Malaysia is a developing nation, boasting two of the world's tallest structures – the Petronas Towers and the Merdeka 101 Tower. The Petronas Towers is an iconic symbol of the city and a marvel of modern architecture. Designed by the Argentine architect Cesar Pelli & Associates and Thorton-Tomasetti Engineers, the Petronas Towers were inspired by Islamic art and culture. The towers' design drew inspiration from the traditional motifs and Islamic geometric patterns, rendering a fine blend of modern and cultural elements.

The Petronas Towers, standing at a height of 452 meters, features two identical towers of 88 floors above ground and five below ground, connected by a skybridge on the 41st and 42nd floors, holding the record for the highest 2-story bridge in the world. The skybridge also functions as a crucial design feature facilitating movement between the two towers during high winds. The bridge is 170 m (558 ft) above the ground and 58.4 m (192 ft) long, weighing 750 tons.

The construction of the Petronas Towers was a massive undertaking that required the collaboration of architects, engineers, and builders from around the world. The towers were built using the "slipform" technique.

The towers were built on a soft soil foundation, which posed a significant engineering challenge. The foundation system consisted of a 4.5-meter-thick piled raft supported on rectangular friction piles, varying in depth from 40 meters to 105 meters and each foundation consisted of 104 barrettes.

The height of the Petronas Towers made them vulnerable to wind forces. In addition to the challenges of building and maintaining the Petronas Towers, the towers also had to be designed to withstand earthquakes.

Though the country due to its locations has been conventionally perceived as an earthquake-free zone, numerous reports highlight that Malaysia has experienced number of earthquakes, mainly due to the fault sources in Indonesia and the Philippines. Small earthquakes with moment magnitudes less than 5 have been recorded within the Peninsular Malaysia and Sarawak regions. Unfortunately, in 2015, a magnitude 6.0 earthquake struck Ranau, Sabah, causing considerable damage to several buildings, marking it as a case of moderate seismicity.

They were built to withstand earthquakes up to a magnitude of 7.5 on the Richter scale. The towers' design included a system of steel braces and concrete walls that help to absorb and dissipate seismic energy, making them one of the safest buildings in the world during an earthquake.

The structure of the building comprised of a dual system consisting of reinforced concrete core wall system and exterior reinforced concrete column. The floor framing system consisted of composite steel framing system. A composite metal deck framed between the steel beams to act compositely with them. The structural frame for each of the main towers consisted of sixteen cylindrical high-strength concrete perimeter columns connected by a haunched ring beam at each level. This allowed for the passage of mechanical systems at the centre span of the beam. This frame is tied back to the structural elevator core at the thirty-eighth and fortieth floors by concrete outrigger beams.

The core was constructed with added strength at the corners to help resist the moment created by lateral forces. Two shear walls cross with the core to further enhance the stiffness. The grade of concrete ranges from 80 MPa at the base to 40 MPa at the top.

The columns varied in size from 2.4 m diameter at the base to 1.2 m diameter at the top and were placed at the outside corners. The columns were linked with a series of concrete core walls and ring beams. There were two concentric pressurized cores in the structures and they unite at the 38th floor of each tower.

The Petronas Towers stand tall as a testament to human ingenuity, architectural excellence, and cultural significance. With their iconic design, innovative engineering, and sustainable features, they have left an indelible mark on the global architectural landscape. The towers serve as a symbol of Malaysia's aspirations and achievements, capturing the imagination of visitors and inspiring awe in all who behold their majestic presence.

REFERENCES

1. MALAYSIA'S EARTHQUAKE STRUGGLE: NAVIGATING THE PATH TO RESILIENCE IN BUILDING SAFETY
2. https://iopscience.iop.org/article/10.1088/1742-6596/2287/1/012026/pdf
3. DESIGN + STRUCTURE - PETRONAS Twin Towers
4. Exploring the Petronas Towers: Twin Skyscrapers and Modern Landmark in Kuala Lumpur - WeChronicle
5. Petronas Towers | PPT
6. Petronas Towers: A Towering Architectural Triumph - DesignAsia Magazine
7. The Petronas Towers, Kuala Lumpur, Malaysia, 1998. | Download Scientific Diagram
8. PETRONAS TWIN TOWERS || ENGINEERING ASPECTS
9. A comprehensive introduction to outrigger and belt-truss system in skyscrapers - ScienceDirect

HANDBOOK ON PRECAST CONCRETE FOR BUILDINGS – A PRIMER

Amlan K. Sengupta
Professor
Indian Institute of Technology Madras

INTRODUCTION

The use of precast concrete is considered to be a solution for the construction of mass housing in India. Though this technology has been in use in India for several decades, it is not utilised substantially because of a few impediments. The Ministry of Housing and Urban Affairs has recently launched 'Global Housing Technology Challenge – India' (www.ghtc-india.gov.in), in which precast concrete technology is considered to be one proven technology [1]. The Indian Concrete Institute published the Handbook on Precast Concrete for Buildings [2] (Figure 1) with the objective to cover wide ranging topics of precast concrete,
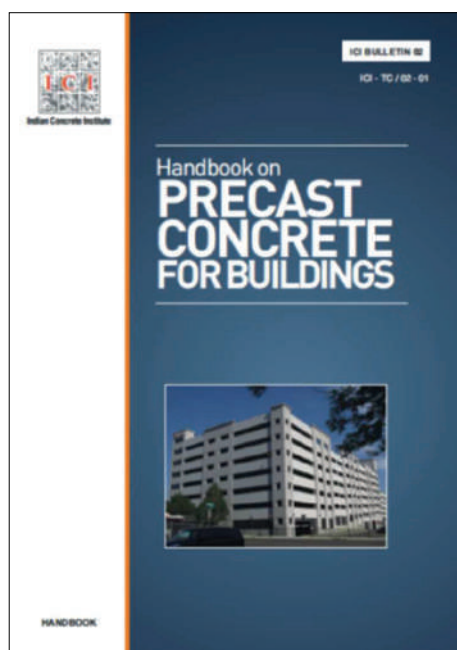

Fig. 1: Cover of the Handbook on Precast Concrete for Buildings

with a simple to read and easy to comprehend approach. To maintain brevity, information that is commonly used in design and construction of reinforced concrete structures was not covered. There are references in the handbook which can be accessed for additional material. The different chapters of the handbook were authored by professionals from the construction industry, scientists from a research organisation, and academicians involved in education and research related to precast concrete. This paper briefly presents the content of the handbook chapter wise.

The Bureau of Indian standards had published codes on precast concrete ([3] to [8]). These are listed under References as a source of information. A new comprehensive code will be published which will cover materials, structural systems, analysis and design, planning and construction, quality assurance etc.

DESCRIPTION OF THE CHAPTERS

The chapters are explained briefly.

PRECAST CONCRETE IN BUILDINGS

The benefits of precast concrete can be summarised under the following categories.

- Quality
  - Better control in a factory environment
  - Suitable during inclement weather
  - Efficient quality management
  - Accuracy in dimensions
  - Possibility of textured finish
- Time
  - Rapid construction with robust planning
  - Use of mechanised ways, such as extrusion, battery and tilting moulds etc.
  - Suitable for modular and repetitive construction
- Cost
  - Optimum use of materials
  - Limited use of temporary supporting structures, such as scaffolding
  - Multiple use of form work
  - Availability of standard shapes
  - Reduced maintenance leads to reduced life-cycle cost

However, there are challenges in adopting precast concrete technology. These can be as follows.

- High initial costs for setting up factories
- High transportation costs for delivery of precast components
- Erection of components
- Excise duty of precast products

The chapter provides the potential for use of precast concrete, with reference to the developments in other countries which are advanced in this technology. The special types of form work that can be used are large area forms, wall forms, climbing forms, slip forms, automatic hydraulic forming systems, heated tunnel forms etc. Large projects undertaken in the past are highlighted.

PRECAST CONCRETE BUILDING SYSTEMS – AN OVERVIEW

There are different types of precast concrete buildings and hence, it is necessary to classify them for better understanding. In this chapter, the different systems and sub-systems adopted in precast concrete buildings are elucidated, namely overall structural systems, systems for lateral load resistance, roof and floor systems. The systems are illustrated using photos of constructed facilities.

The structural system refers to the combination of the primary components of a building that resist the loads acting on the building. First, the different types of systems to resist the gravity loads are presented under overall structural systems. The systems are classified as follows.

- Skeletal frame system (Figure 2)
- Large panel (wall) system (Figure 3)
- Cell (3D volumetric) system

Second, the systems to resist the lateral loads due to earthquake and wind, are grouped as low-rise portals and frames, multi-storeyed frames, and wall system. The roof and floor systems are presented separately to explain the transfer of loads between the several components.

The different types of individual precast components for buildings are also described briefly. These include beams, columns, and units for the roofs, floors, walls and foundations.

Comparative statements relating to suitable spans and material consumption are tabulated for ready reference.

Fig. 2: Framed system: Terminal building at Bangalore airport

Fig. 3: Large panel system: High-rise apartment buildings at Mumbai

FOUNDATION AND UNDER-GROUND STRUCTURES

Precast concrete can be adopted both for shallow foundations such as individual pad footings, and deep foundations such as piles. Apart from the general advantages, the advantages of adopting precast concrete for the foundations are as follows.

- The foundation stratum is exposed for a minimum period. The backfilling can be carried out immediately after placing the footing component.
- The excavation size can be reduced.

However, the connection of the superstructure with the foundation needs appropriate detailing. The chapter provides for the pad footings and the piles. Apart from the building structures, precast concrete can be used for other underground structures such as pipes, drains, culverts, tunnels, in-take wells etc. Precast concrete is extensively used in other geo-structures such as facial elements in reinforced earth walls, interlocking blocks in pavements, liner elements in canals and water reservoirs.

STRUCTURAL ANALYSIS AND DESIGN

The structural analysis and design of precast concrete buildings follow the same principles as used in conventional construction. However, attention is required to model the structure appropriately considering the behaviour of the joints of the members. The modelling of the joints should be based on the adopted type of design. First, the chapter provides an overview of the loads based on the provisions of the Indian codes IS 875 Parts 1 to 3, and IS 1893 Part 1. Next, the analyses of frames are presented for a few typical types of frames. The design and detailing for the tie reinforcement required to avoid progressive collapse, is highlighted.

PRESTRESSED PRECAST CONCRETE

The major advantages of prestressing precast concrete members in buildings are as follows.

- The span-to-depth ratio of a flexural member can be increased. With reduced depth, the amount of concrete and self-weight decrease. The section tends to be aesthetically appealing. There can be large column-free space.
- Under service conditions, the members can remain uncracked. This leads to increase in section stiffness and durability. The shear capacity near the supports also increases.

The common applications of prestressing are hollow core slabs, composite slabs, beams, double tee girders, folded plate and shell members, roof trusses, piles and miscellaneous components. However, the limitations for prestressing include the availability of prestressing bed or self-straining

> **The structural analysis and design of precast concrete buildings follow the same principles as used in conventional construction.**

benches, auxiliary equipments, good quality material and skilled labour.

The chapter provides the essentials of the analysis, design and construction of prestressed members.

SEISMIC DESIGN OF PRECAST STRUCTURES

The failures of precast concrete structures in past earthquakes have raised concern of the use of such structures in earthquake prone areas. It has been observed that the failures are primarily triggered by those at the joints of the precast components. The seismic design of a precast structure covers the overall seismic analysis of the structure, the design of the components, the detailing of the joints and providing integrity reinforcement. The first two aspects are similar to those of conventional reinforced concrete structures.

There are two basic approaches for the detailing of the joints.

- Emulative or wet joints
- Mechanical or dry joints

In the wet joints, reinforcement protrudes from the adjacent components, and on site concrete or grout is used to connect the components. The design aims to emulate or mimic the behaviour of cast-in-place construction. On the contrary, dry joints consist of metallic connectors with adequate corrosion protection.

The chapter first covers the basics of seismic analysis and design of buildings. Next, the detailing of joints is covered based on the different types of components to be connected. The detailing for slabs as floor diaphragms is also provided.

MATERIALS, PROPERTIES AND PRODUCTS

The common materials used in making concrete are aggregates, cement, supplementary cementitious materials, chemical and mineral admixtures, and water. Reinforcing bars, prestressing strands, welded wire mesh and splice sleeve couplers are used as reinforcement. Ducts, grouts, dry packs, looped wire ropes, metallic inserts and plates are used in the joints. The selection of materials with appropriate properties is necessary for the mechanised manufacturing of the precast

components. A few important requirements of precast concrete are as follows.

- Early high strength for release of the components from the moulds
- High flow mix or even self compacting concrete in case of components with dense reinforcement.
- Stiff mix to facilitate extrusion in hollow core slabs and finishing in flat works

Special types of concrete are used based on the applications, such as coloured concrete, textured concrete, light weight concrete, high performance concrete, aerated concrete, etc. Sandwich wall panels with expanded or extruded polystyrene are used for thermal insulation. Typically, the cast components are subjected to accelerated curing, such as steam curing, electrical resistance curing or hot air/water curing.

JOINTS AND CONNECTIONS IN PRECAST BUILDINGS

A 'joint' in a structure is defined as the junction between the members. The 'connection' includes elements (eg. bars, plates, etc.) used in a joint. As mentioned under seismic design, that joints are the vulnerable parts of a precast concrete structure. The chapter describes the design of joints based on the flows of forces that arise in the different types of members to be connected.

- Column to foundation
- Column to column
- Beam to column
- Slab to beam
- Slab to slab
- Panel to panel

There is a section on components in joints such as couplers, dowels, headed studs, bolts, inserts and bearing pads.

PRODUCTION, HANDLING AND ERECTION OF PRECAST ELEMENTS

The setting up of a factory for production of precast concrete components needs careful planning. The common types of moulds that are used for precast concrete are as follows.

- Column moulds: with or without corbels
- Beam moulds
- Wall moulds: flat/table moulds, vertical moulds, battery moulds, tilting moulds

> ## " The setting up of a factory for production of precast concrete components needs careful planning. "

- Slab moulds: hollow core slab bed moulds, plank moulds
- Staircase moulds
- Moulds for miscellaneous non-structural components

The chapter describes the moulds and their tolerances. The typical production process is explained using a flow chart. Equipment for curing, storage, transportation, handling and erection are briefly presented. The installations of various components are described.

QUALITY CONTROL AND ASSURANCE IN PRECAST PRODUCTS

The chapter provides the aspects of quality control of raw materials and their storage, production process, the finished products and the testing procedures.

CONTRACTS AND TAXATION

First, the chapter briefly describes the general types of contracts.

- Item rate contract
- Lump sum or Design-and-build contract
  - Turn-key contract
  - Engineering Procurement and Construction (EPC) contract
- Cost-plus contract

Considering lean construction concepts, the following variants are possible.

- Target Value Design
- Integrated Project Delivery
- Alliance Contracting

Next, the chapter provides the aspects of contracts that are relevant to precast concrete construction. The taxation system for precast concrete construction in India is covered.

INFORMATION TECHNOLOGY IN PRECAST CONSTRUCTION

The use of Building Information Modelling (BIM) in precast concrete construction is described under the following sections.

- Creating a conceptual model and generation of tender quantities
- Integration with analysis and design applications
- Precast member connections and detailing
- Creating of drawings, reports and bill of materials
- Change management
- Generating automated deliverables
- Automated detailed drawings
- Site and delivery scheduling
- Field erection

CASE STUDIES

Two case studies are provided to elucidate the various aspects of the design of precast concrete structures.

- Canteen building constructed for an information technology hub (Figure 4)
- Multi-level vehicular parking garage for an international airport (Figure 5)

The architectural layout, structural systems, structural analysis models, adaptation of precast system, components used and the

Fig. 4: Case Study 1: Canteen building with hollow core slab system

Fig. 5: Case Study 2: Multi-level vehicular parking garage

erection scheme for each of the above projects are explained.

CLOSURE

The use of precast concrete leads to better quality, faster and economical construction of buildings. Further development of this industry will provide pre-fabricated pre-finished volumetric construction, as is being adopted in certain countries. The Handbook on Precast Concrete for Buildings is a source of compiled information. For better understanding, it provides several illustrations and sketches. The references in each chapter can be accessed for additional material.

ACKNOWLEDGEMENTS

REFERENCE

1. Alternate and Innovative Construction Systems for Housing (2021), Building Materials and Technology Promotion Council and I. K. International Pvt. Ltd.

2. Handbook on Precast Concrete for Buildings (2018), ICI Bulletin 02, Indian Concrete Institute.

3. IS 10297: 1982, Code of Practice for Design and Construction of Floors and Roofs using Precast Reinforced/Prestressed Concrete Ribbed or Cored Slab Units, Bureau of Indian Standards.

4. IS 10505: 1983, Code of Practice for Construction of Floors and Roofs using Precast Concrete Waffle Units, Bureau of Indian Standards.

5. IS 11447: 1985, Code of Practice for Construction with Large Panel Prefabricates, Bureau of Indian Standards.

6. IS 14213: 1994, Construction of Walls using Precast Concrete Stone Masonry Blocks – Code of Practice, Bureau of Indian Standards.

7. IS 15916: 2010, Building Design and Erection using Prefabricated Concrete – Code of Practice, Bureau of Indian Standards.

8. IS 15917: 2010, Building Design and Erection using Mixed/Composite Construction – Code of Practice, Bureau of Indian Standards.

ADVANCED COMPUTER VISION TECHNIQUES FOR STRUCTURAL HEALTH MONITORING

Subhajit Banerjee
Research Scholar
School of Infrastructure
IIT Bhubaneswar
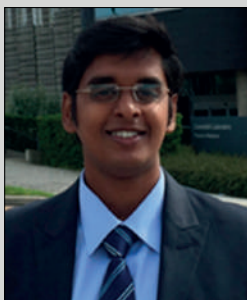
T Jothi Saravanan
Assistant Professor
School of Infrastructure
IIT Bhubaneswar

INTRODUCTION

Key civil infrastructure assets such as bridges, tunnels, railways, roads, and buildings are integral to economic development and the functionality of urban environments [1]. However, these structures are susceptible to progressive degradation, primarily due to environmental exposure, repetitive stress, or unexpected events like natural disasters. Over time, such deterioration can undermine structural integrity, posing latent risks that may escalate to catastrophic failures or operational inefficiencies if not addressed [2]. Routine inspections are essential for ensuring the safety and operational performance of infrastructure. Historically, manual on-site inspections, conducted by trained professionals, have been the primary approach for identifying damage and structural changes. While effective for localized assessments, this method is labour-intensive, time-consuming and impractical for large-scale infrastructure. Additionally, the reliability of such evaluations often depends heavily on the skill and subjective judgment of the inspector, introducing variability into the process.

To address these limitations, structural health monitoring (SHM) has emerged as a transformative solution, leveraging advancements in technology to provide systematic, objective evaluations of structural integrity. SHM systems aim to collect accurate and timely data on structural behaviour, enabling proactive maintenance to avert severe consequences [3]. Traditionally, SHM has relied on contact-based sensors such as accelerometers, strain gauges, fibre-optic sensors, etc. which are directly affixed to the structure, for collection of structural vibration response data [4]. However, the installation and upkeep of these sensors on large-scale structures can be challenging and costly, and their measurements are often limited to localized application points, resulting in incomplete assessments. Furthermore, for smaller structures, the presence of added mass from contact sensors may affect the accuracy of data collected [5]. Sophisticated non-contact sensors such as Laser Doppler Vibrometer (LDV), Microwave Inferometer (MI) with high spatial resolution sensing capability could address some of the above challenges in structural response measurement [6,7]. The extensive use of these advanced vibration recording devices is, however, constrained by a number of factors, including the high cost of the instruments, the labour-intensive installation process, the need for fixed platforms, and their small coverage area, which makes it challenging to obtain precise displacement response data.

The last decade has seen SHM approaches to focus more towards more efficient and practical non-contact sensors, largely driven by recent advancements in innovative technologies. Computer vision (CV)-based solutions have proved to be a promising and potential tool for SHM operations on large scale

structures, owing to recent advancements in optical sensing technologies, such as high-resolution cameras, along with supporting devices like drones and robotic platforms [8-11]. These methods leverage sophisticated image processing frameworks, incorporating machine learning and deep learning algorithms, to provide a robust alternative to traditional manual inspections. Compared to conventional techniques, CV-based systems offer multiple advantages, including non-contact and long-range monitoring capabilities, portability when mounted on vehicles, increased spatial resolution, cost-effectiveness in installation, and automated assessment when integrated with artificial intelligence. These features make them particularly suitable for long-term structural monitoring and for enabling timely maintenance interventions to mitigate risks. CV systems have demonstrated efficacy in evaluating both localized structural conditions (e.g., crack detection, spalling, corrosion, delamination) and global parameters (e.g., vibrational analysis, deformation, and displacement measurements) across diverse SHM applications. Fig. 1(a) and 1(b) demonstrates the percentage distribution of recent studies in advanced vision-based health monitoring solutions for real-life infrastructures, in terms of type of infrastructure addressed and type of SHM implemented, respectively. The following section elaborates some cutting-edge CV techniques that are being utilized in SHM applications.

## STATE-OF-THE-ART COMPUTER VISION TECHNIQUES IN SHM

DISPLACEMENT EXTRACTION AND DEFORMATION MEASUREMENT FROM VIBRATION VIDEO DATA

Optical flow techniques are extensively used as CV techniques to analyze the movement of pixels across sequential image frames to estimate displacement and deformation in structures [13]. Algorithms like Kanade-Lucas-Tomasi (KLT) and Farnebäck are particularly effective in capturing small-scale motions, making them invaluable in SHM applications [14, 15]. These methods identify temporal variations in structural responses, including vibrations caused by environmental or operational loads. Their ability to provide sub-pixel motion accuracy ensures precise assessment of structural integrity. For example, monitoring bridges under dynamic loading conditions can reveal stiffness changes indicative of damage progression. Recent advancements in deep optical flow methods, which incorporate neural networks, have further improved motion estimation in noisy or low-light environments. Large displacement optical flow techniques [16] enable robust estimation of extensive motion fields between image frames, making them particularly suitable for capturing complex motion patterns in large-scale structures under extreme dynamic load conditions.

Digital Image Correlation (DIC) algorithm is also a widely adopted technique that compares surface patterns between reference and deformed states to quantify displacement and
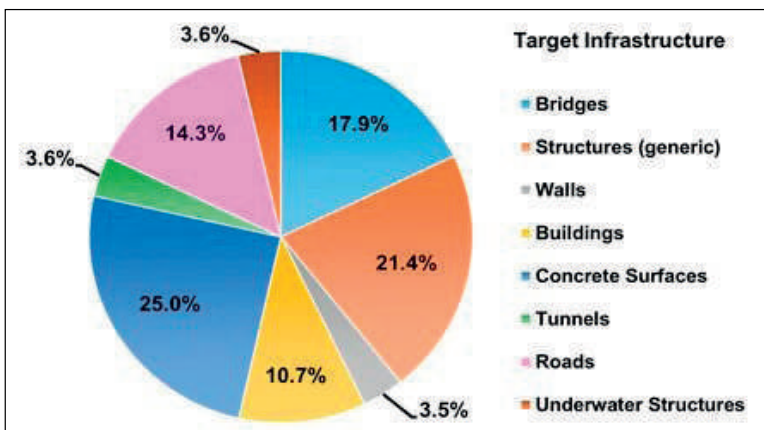
1(a). Percentage distribution showing type of infrastructures studied
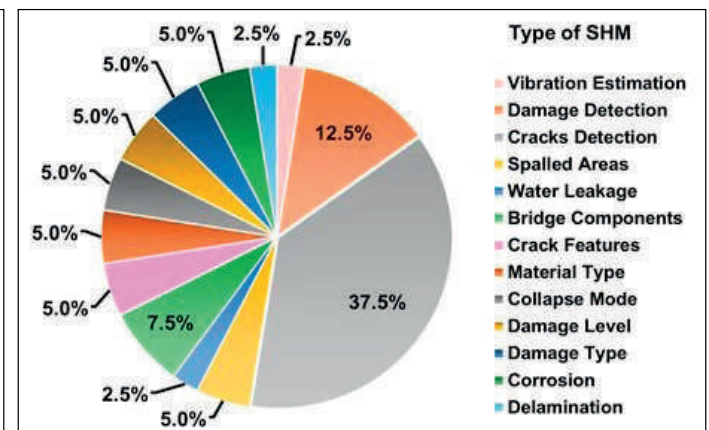
1(b). Percentage distribution showing structural traits monitored

Fig. 1: Percentage distribution charts from CV-based SHM studies performed on real-world structures in recent years [12]

strain [17]. This method is especially useful for assessing material behavior under static and dynamic conditions. High-resolution images of structural elements, such as beams and plates, allow the tracking of minute deformations, offering insights into localized strain distributions. DIC systems are extensively used in laboratory experiments and field applications for crack propagation studies, fatigue analysis, and performance evaluation of structural materials [18]. Their non-invasive nature makes them ideal for use in delicate or heritage structures.

Phase-based video motion estimation (PBVME) amplifies imperceptible structural vibrations captured in video recordings, enabling precise estimation of modal parameters like natural frequencies and mode shapes [19, 20]. By isolating phase information from video data, this technique detects subtle oscillations, even in low-amplitude vibrations. Its application in SHM includes identifying resonant frequencies of bridges or towers, which can indicate changes in structural stiffness or mass distribution. This approach is computationally efficient and cost-effective, requiring only a standard video camera and minimal post-processing resources.

DAMAGE DETECTION USING STOCHASTIC SUBSPACE ANALYSIS

Stochastic subspace analysis has emerged as a sophisticated technique for vibration-based damage detection in SHM, particularly when applied to real-world structures where input excitation is unknown (stochastic) [21]. This technique utilizes the stochastic nature of structural damage which arises from uncertain loading conditions, variability in material characteristics. It involves extracting the state-space matrices of the structural system in both damaged and reference (undamaged) states, and detect the deviations in the state of the system indicating potential damage.

Stochastic Subspace Identification (SSI) [22] is a powerful algorithm for identifying state-space models of structures based on vibration data. By analyzing ambient or forced vibration responses, SSI estimates modal parameters such as natural frequencies, damping ratios, and mode shapes without requiring predefined

> **By isolating phase information from video data, this technique detects subtle oscillations, even in low-amplitude vibrations.**

input excitation. In damage detection, SSI is used to derive state matrices from vibration displacement data collected under operational conditions. Changes in these matrices, such as shifts in eigenvalues or mode shapes, serve as indicators of structural damage. SSI's robustness to environmental variability makes it ideal for long-term monitoring of bridges, buildings, and other infrastructure.

Stochastic Damage Locating Vectors (SDLVs) [23-25] are fictitious static load vectors computed from the state-space matrices of undamaged and damaged states of the structure, that have a unique property of inducing zero magnitude stress fields in the damaged structural elements when applied on the finite element model of the structure. This method is particularly effective for isolating damage in complex systems where traditional methods may struggle.

DEEP LEARNING FOR STRUCTURAL DAMAGE DETECTION

Convolutional Neural Networks (CNNs) excel in feature extraction and classification tasks, making them ideal for SHM. They are extensively used for detecting surface cracks, spalling, and corrosion in concrete and steel structures [26]. Models like ResNet, YOLO, and Faster R-CNN [27-30] enable real-time analysis of structural images and videos, offering high accuracy in damage classification. Pretrained networks fine-tuned on structural datasets further enhance detection capabilities, even under variable lighting or environmental conditions. CNNs also support multi-scale

feature extraction, critical for identifying both micro- and macro-level damages.

Generative Adversarial Networks (GANs) are employed to augment training datasets by simulating diverse structural damage scenarios [31]. This improves model robustness against real-world complexities. GANs generate high-resolution synthetic images depicting various types of defects, such as cracks of different shapes and orientations. These datasets are then used to train CNNs and other deep learning models, enhancing their ability to generalize across diverse damage patterns.

Transformers have recently gained attention in SHM for their ability to handle large-scale sequential data [32]. Vision Transformers (ViTs) [33] offer state-of-the-art performance in image and video analysis tasks, outperforming CNNs in many cases. They are particularly effective in analyzing long-range dependencies in time-series data, making them suitable for vibration monitoring and anomaly detection in SHM.

NOVELTY AND ANOMALY DETECTION

Unsupervised learning methods are increasingly adopted for identifying unusual patterns in SHM data. Clustering algorithms, such as K-Means and Gaussian Mixture Models [34], help segment vibration data into clusters, highlighting outliers that may indicate damage. Autoencoders, a type of neural network, learn normal structural behavior and flag deviations as potential anomalies. Principal Component Analysis (PCA) reduces the dimensionality of SHM datasets, simplifying the identification of abnormal trends in structural response [35]. These approaches are particularly valuable for long-term monitoring, where damage patterns may evolve gradually over time.

> **The integration of Digital Twin (DT) technology with CV-based SHM shows potential as a transformative approach to infrastructure management.**

3D RECONSTRUCTION AND SHAPE ANALYSIS

3D reconstruction techniques [36, 37] such as 3D point cloud generation can provide detailed geometric representations of structures, enabling the detection of shape anomalies and deformations. This approach is critical for assessing complex structures like bridges, dams, and historical monuments, where geometric changes can signal underlying issues. Advanced 3D reconstruction frameworks also support integration with digital twin technologies, providing real-time updates on structural health.

INTEGRATION WITH ROBOTICS AND IOT

Robotics and IoT technologies enhance the efficiency and accessibility of CV-based SHM systems [8, 9]. Drones equipped with high-resolution cameras enable aerial inspections of bridges, towers, and dams, reducing the risks associated with manual inspections [11]. Autonomous ground vehicles provide close-range imaging of structural elements, including those in hazardous areas. IoT integration allows for real-time data processing through edge computing, minimizing latency and bandwidth requirements. These systems support continuous monitoring, enabling proactive maintenance strategies and reducing downtime.

FUTURE SCOPE OF UTILIZATION OF ADVANCED CV FOR SHM

DIGITAL TWIN INTEGRATION

The integration of Digital Twin (DT) technology with CV-based SHM shows potential as a transformative approach to infrastructure management. By combining real-time CV data with predictive simulation models, DTs can provide an accurate virtual replica of a structure, enabling proactive maintenance strategies. This integration enhances damage prediction and allows for optimal decision-making by continuously updating the virtual model with visual data, such as crack progression or displacement changes, for real-time analysis.

QUANTUM COMPUTING

Implementation of CV-based techniques for real-time SHM applications often require

substantial processing power, necessitating advancements in GPU-based and distributed computing. Quantum computing holds potential to revolutionize the processing capabilities of CV-based SHM systems, particularly when handling large volumes of high-dimensional data. The inherent parallelism of quantum processors allows for faster computations, enabling more efficient analysis of complex data sets such as 3D structural scans or multi-modal vibration data. Quantum algorithms could significantly speed up the processing of imaging data, anomaly detection, and optimization tasks, thus improving the real-time capabilities of SHM systems. Although still in its early stages, quantum computing's ability to handle vast amounts of data with unprecedented speed will be critical as SHM systems evolve to manage ever-increasing data complexity.

CONCLUSION

Advanced computer vision techniques are redefining the scope of structural health monitoring by offering innovative, non-invasive, and scalable solutions. The integration of CV with AI, robotics, and IoT has demonstrated its potential to address critical SHM challenges, ensuring infrastructure safety and resilience. With continuous advancements in imaging technologies and computational methods, CV-based SHM systems are poised to play a pivotal role in the proactive management of critical structures, while paving the way for innovative applications in engineering.

REFERENCES

1. Thacker, S.; Adshead, D.; Fay, M.; Hallegatte, S.; Harvey, M.; Meller, H.; O'Regan, N.; Rozenberg, J.; Watkins, G.; Hall, J.W. Infrastructure for sustainable development. Nat. Sustain. 2019, 2, 324–331.

2. Frangopol, D.; Soliman, M.S. Life-cycle of structural systems: Recent achievements and future directions. Struct. Infrastruct. Eng. 2016, 12, 1–20.

3. Li, H.-N.; Ren, L.; Jia, Z.-G.; Yi, T.-H.; Li, D.-S. State-of-the-art in structural health monitoring of large and complex civil infrastructures. J. Civ. Struct. Health Monit. 2015, 6, 3–16.

4. Fan, W. and Qiao, P. (2011): Vibration-based damage identification methods: a review and comparative study. Structural health monitoring, 10(1), 83–111.

5. Ashory, M. (1998): Correction of mass-loading effects of transducers and suspension effects in modal testing. In: Proceedings of the 16th International Modal Analysis Conference, 3243.

6. Farrar, C. R., Darling, T. W., Migliori, A., and Baker, W. E. (1999): Microwave interferometers for non-contact vibration measurements on large structures. Mechanical Systems and Signal Processing, 13(2), 241–253.

7. Saravanan, T. J., Gopalakrishnan, N., and Rao, N. P. (2015). Damage detection in structural elements through propagating waves using radially weighted and factored RMS. Measurement, 73, 520–538.

8. Poorghasem, S.; Bao, Y. Review of robot-based automated measurement of vibration for civil engineering structures. Measurement 2023, 207, 112382.

9. Tian, Y.; Chen, C.; Sagoe-Crentsil, K.; Zhang, J.; Duan, W. Intelligent robotic systems for structural health monitoring: Applications and future trends. Autom. Constr. 2022, 139, 104273.

10. Ye, X.W.; Dong, C.Z.; Liu, T. A Review of Machine Vision-Based Structural Health Monitoring: Methodologies and Applications. J. Sens. 2016, 2016, 7103039.

11. Carroll, S.; Satme, J.; Alkharusi, S.; Vitzilaios, N.; Downey, A.; Rizos, D. Drone-Based Vibration Monitoring and Assessment of Structures. Appl. Sci. 2021, 11, 8560.

12. Ferraris, C.; Amprimo, G.; Pettiti, G. Computer Vision and Image Processing in Structural Health Monitoring: Overview of Recent Applications. Signals 2023, 4, 539-574.

13. Niu, Y., Li, Z., Li, J., & Sun, B. (2025). Accelerometer-assisted computer vision data fusion framework for structural dynamic displacement reconstruction. Measurement, 242, 116021.

14. Chang, C. M., & Chou, J. Y. (2023). Deformation estimation of truss bridges using two-stage optimization from cameras. Smart Structures and Systems, An International Journal, 31(4), 409-419.

15. Kim D-H, Gratchev I. Application of Optical Flow Technique and Photogrammetry for Rockfall Dynamics: A Case Study on a Field Test. Remote Sensing. 2021; 13(20):4124.

16. Z. Chen, H. Jin, Z. Lin, S. Cohen and Y. Wu, "Large Displacement Optical Flow from Nearest Neighbor Fields," 2013 IEEE Conference on Computer Vision and Pattern Recognition, Portland, OR, USA, 2013, pp. 2443-2450.

17. Saravanan, T. J., Gopalakrishnan, N., and Hari, B. K. (2019). Damage identification in structural elements through curvature mode shapes and nonlinear energy operator. Compos. Mater. Engg., 1(1), 33–48.

18. Ziaja, D., Jurek, M., Śliwa, R., Wiater, A., & Kulpa, M. (2024). DIC application for damage detection in FRP composite specimens based on an example of a shearing test. Archives of Civil and Mechanical Engineering, 24(1), 47.

19. Wadhwa, N., Rubinstein, M., Durand, F., and Freeman, W. T. (2013): Phase-based video motion processing. ACM Transactions on Graphics (TOG), 32(4), 1–10.

20. Chen, J. G., Wadhwa, N., Cha, Y.J., Durand, F., Freeman, W. T., and Buyukozturk, O. (2015): Modal identification of simple structures with high-speed video using motion magnification. Journal of Sound and Vibration, 345, 58–71.

21. Van Overschee, P., & De Moor, B. (1994). N4SID: Subspace algorithms for the identification of combined deterministic-stochastic systems. Automatica, 30(1), 75-93.

22. Shokravi, H., Shokravi, H., Bakhary, N., Rahimian Koloor, S. S., & Petrů, M. (2020). Health monitoring of civil infrastructures by subspace system identification method: An overview. Applied Sciences, 10(8), 2786.

23. Bernal, D. (2006): Flexibility-based damage localization from stochastic realization results. Journal of Engineering Mechanics, 132(6), 651–658.

24. Bernal, D. (2010). Load vectors for damage location in systems identified from operational loads. Journal of engineering mechanics, 136(1), 31-39.

25. Marin, L., Döhler, M., Bernal, D., & Mevel, L. (2015). Robust statistical damage localization with stochastic load vectors. Structural Control and Health Monitoring, 22(3), 557-573.

26. Kord, S., Taghikhany, T., & Akbari, M. (2024). A novel spatiotemporal 3D CNN framework with multi-task learning for efficient structural damage detection. Structural Health Monitoring, 23(4), 2270-2287.

27. Wang, R., Zhou, X., Liu, Y., Liu, D., Lu, Y., & Su, M. (2024). Identification of the Surface Cracks of Concrete Based on ResNet-18 Depth Residual Network. Applied Sciences, 14(8), 3142.

28. Huang, C., Zhou, Y., & Xie, X. (2024). Intelligent Diagnosis of Concrete Defects Based on Improved Mask R-CNN. Applied Sciences, 14(10), 4148.

29. Jothiraj, S., Balu, S., Rengarajan, N., & Nagarani, N. (2024). Monitoring Ancient Buildings Using UAV and Instant Image Segmentation Using Masked R-CNN. In Artificial Intelligence for Multimedia Information Processing (pp. 3-17). CRC Press.

30. Samarin, A., Mamaeva, A., Toropov, A., Dzestelova, A., Kotenko, E., Nazarenko, A., ... & Motyko, A. (2024, October). Wind Turbines Surface Damage Automatic Detection Using YOLOv8 with Specialized Backbone Modification. In 2024 36th Conference of Open Innovations Association (FRUCT) (pp. 702-710). IEEE.

31. Shim, S. (2024). Self-training approach for crack detection using synthesized crack images based on conditional generative adversarial network. Computer-Aided Civil and Infrastructure Engineering, 39(7), 1019-1041.

32. Azimi, M., & Yang, T. Y. (2024). Transformer-based framework for accurate segmentation of high-resolution images in structural health monitoring. Computer-Aided Civil and Infrastructure Engineering.

33. Qin, S., Qi, T., Deng, T., & Huang, X. (2024). Image segmentation using Vision Transformer for tunnel defect assessment. Computer-Aided Civil and Infrastructure Engineering.

34. Fang, F., Ouyang, L., Meng, Y., Xu, Q., Chen, J., & Qiu, L. (2024). Structural adaptive damage detection under uncertainty based on probability dissimilarity and moving average control chart. Measurement, 225, 114023.

35. Nie, Z., Li, F., Li, J., Hao, H., Lin, Y., & Ma, H. (2024). Baseline-free structural damage detection using PCA-Hilbert transform with limited sensors. Journal of Sound and Vibration, 568, 117966.

36. Kim, G., & Cha, Y. (2024). 3D Pixelwise damage mapping using a deep attention based modified Nerfacto. Automation in Construction, 168, 105878.

37. Shi, M., Kim, H., & Narazaki, Y. (2024). Development of large-scale synthetic 3D point cloud datasets for vision-based bridge structural condition assessment. Advances in Structural Engineering, 13694332241260077.

POST-REPAIR ASSESSMENT OF LOAD-CARRYING CAPACITY OF THE ASHULIA BRIDGE

Raquib Ahsan
Ph.D. Professor
Department of Civil Engineering
Bangladesh University of
Engineering and Technology

Md. Rifat Bin Ahmed Majumdar
Graduate Research Assistant
Bangladesh University of
Engineering and Technology

Sadia Sabrin
Graduate Research Assistant
Bangladesh University of
Engineering and Technology

INTRODUCTION

The Ashulia Bridge, over the Turag River on the Tongi-Ashulia-Zerabo-EPZ Road (N302), is a critical structure for the regional connectivity of Dhaka, Bangladesh. Constructed in 1997, the bridge spans 191.5 meters, divided into five equal spans of 38.30 meters each with a width of 10.97 meters. Fig. 1 shows the bridge's top and side views. The plan and cross-sectional views of a span are shown in Figures 2 and 3.

On June 12, 2024, the Ashulia Bridge sustained significant damage following a collision with a sand carrier bulkhead ship. Incident reports highlighted the severe damage to one of the bridge's girders. In response, the bridge authority engaged a contractor to assess the damage and devise a comprehensive strategy for repairing. A detailed inspection subsequently revealed additional damage across multiple spans, necessitating a full-scale repair process to address these structural deficiencies. Moreover, records from the bridge authority's database indicated that the overall condition of the structure

Fig. 1: (a) Top and (b) side view of the bridge
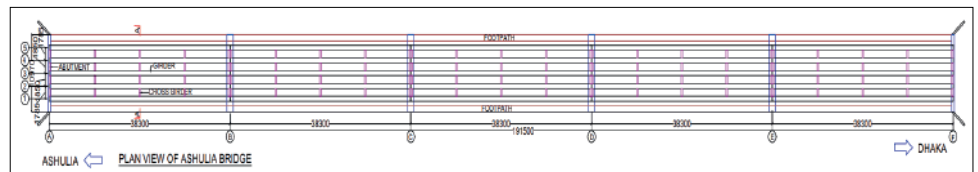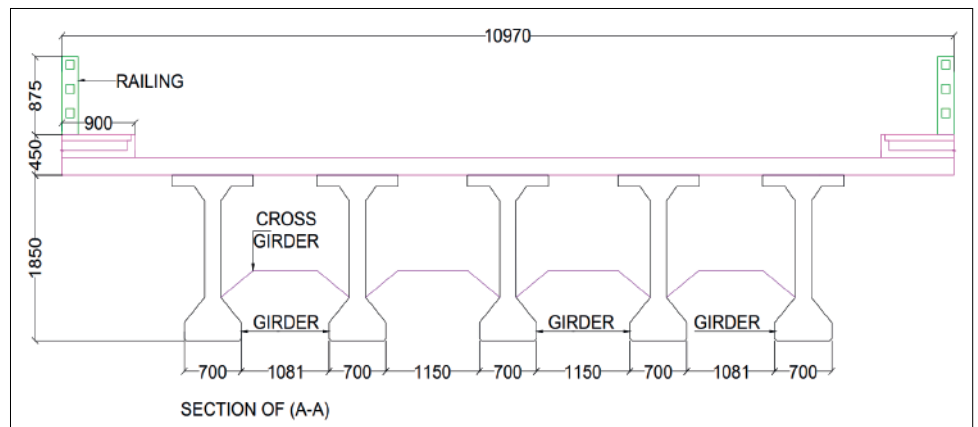

Fig. 2: Plan view of the bridge

Fig. 3: Cross-sectional view of the span

was unsatisfactory, with repairs required for several components.

Considering the concurrent construction of an elevated expressway in this corridor, the Ashulia Bridge is intended to remain operational only as a temporary measure until the expressway becomes functional. Upon completion of the expressway, the bridge will be decommissioned and demolished. Therefore, the primary aim of the repairs was to ensure the bridge's usability and safety during this interim period.

Following the repair process, a comprehensive load test was conducted to evaluate the structural response and determine the maximum permissible load capacity for vehicular traffic. This testing provided critical data to assess whether the retrofitted structure could support expected service loads while meeting safety criteria. Fig. 4 shows photos of the under-construction elevated expressway adjacent to the bridge.

Fig. 4: Elevated expressway pier construction is seen at the background (Photo taken from Ashulia Bridge)

EXTENT OF DAMAGE

The first girders on the north side sustained severe damage due to a collision with an over-height navigation vehicle. Fig. 5 shows different views of the damage. Significant concrete spalling occurred on the first girder near mid-span, exposing internal reinforcement and tendons. Similar spalling was also observed on

Fig. 5: Extent of damage from the field observation
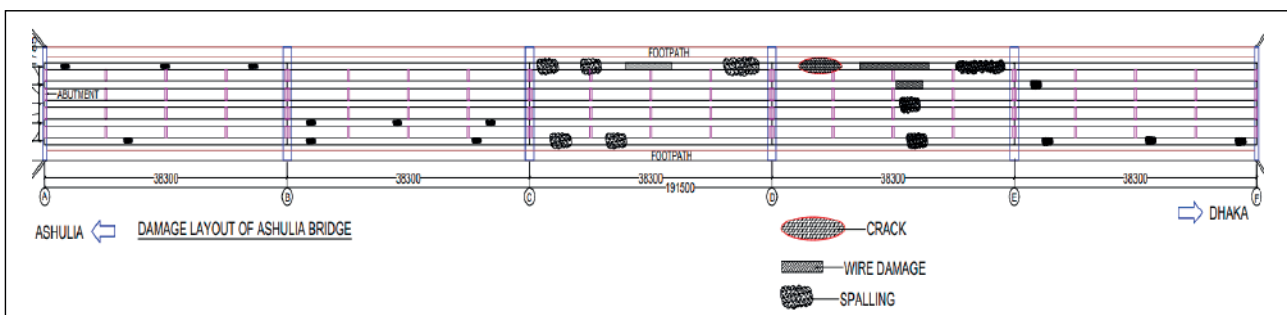
Fig. 6: Schematic view of the damage and cracking of the concrete

the fifth girder. Fig. 6 shows the locations of the concrete damage and associated cracks on the bridge.

REPAIR PLAN AND PROCEDURE

The bridge repair process is explained below:

- **Step 1 (Suspended Staging):** A suspended scaffolding has been installed beneath the bridge to facilitate repair and load testing work. Fig. 7 shows the suspended staging for under-bridge repairs.

Fig. 7: Suspended Staging for Under-Bridge Repairs

- **Step 2 (Repair of Cracks and Spalling of Girder and Pier Cap):** The repair of spalling in the girder and pier cap was carried out using patch repair mortar or micro-concrete. The process began by identifying spalling locations and chipping out all loose concrete. The rebar was then inspected for corrosion; if corrosion was found, section loss was checked. If the section loss was below 20%, the rebar was retained; otherwise, it was replaced with a new rebar. Concrete behind the corroded rebar was removed, ensuring at least 20 mm was cleared, and rust was cleaned from all sides of the rebar while confirming any diameter loss. A zinc-rich coating was applied to prevent further corrosion. For repairs less than 50 mm thick, repair mortar was used, and for repairs greater than 50 mm, formwork was installed, and micro-concrete was applied. Figures 8 and 9 show crack repair using epoxy injection and spalling repair with micro-concrete, respectively.

Fig. 8: Crack Repair by Epoxy Injection

Fig. 9: Spalling repair using Micro-Concrete

- **Step 3 (Strengthening):** The girder strengthening involved the application of six single-layer CFRP laminates to the outer surface of the damaged girder on span 2, covering approximately two-thirds

of the span (around 25 meters). In Fig. 10, FRP strengthening using fiber lamination and fiber wrapping is shown in the plan and girder section.

For CFRP lamination, 210/3300-grade plies were used, each with a thickness of 1.4 mm, an elongation of 1.4%, and a single ply width of 80 mm. The elastic modulus (E_f) is 210 GPa, and the ultimate tensile strength (F_{uf}) is 3.3 GPa, with a fiber content of 70%. Fig. 11 shows the strengthening of the girder through the installation of CFRP laminates.

For CFRP wrapping, 230-grade CFRP was employed, with an elastic modulus (E_f) of 230 GPa, an ultimate tensile strength (F_{uf}) of 4.9 GPa, and an elongation of 1.5%. The ply thickness is 0.112 mm. Fig. 12 illustrates the strengthening of the girder through the installation of CFRP fiber wrapping.

Fig. 12: Strengthening of the girder by installing CFRP fiber wrapping.

LOAD TEST METHODOLOGY

The load test involved measuring acceleration data of the bridge under ambient vibration, vibration due to known vehicular loading, and an impact force. The natural frequency of the

(a)
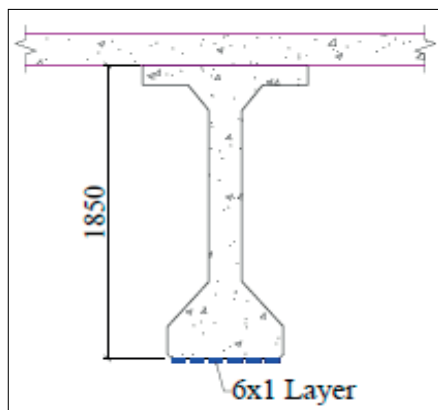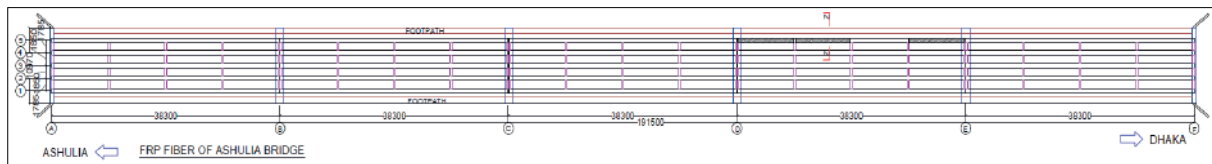
(b)

Fig. 10: (a) The plan and (b) girder section show FRP strengthening through fiber lamination and fiber wrapping
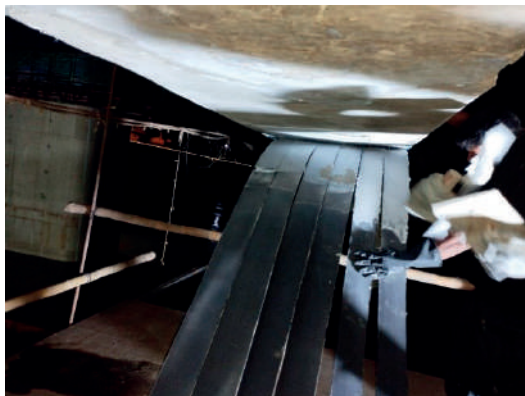
Fig. 11: Strengthening by Installing CFRP Laminates

bridge was estimated from the acceleration data. The natural frequency was then compared to simulations of the bridge model developed using the finite element method. Additionally, the maximum concrete strain resulting from the impact load, as measured by strain gauges, was compared with the strain values predicted by the bridge model.

Once the bridge model was validated, a time history analysis was performed using specified truckloads. Subsequently, the bridge was evaluated against the AASHTO standard HL-93K truckload to assess whether it meets the necessary conditions for structural adequacy.

LOAD TESTING DESIGN AND IMPLEMENTATION

Unidirectional Integrated Circuit Piezoelectric (ICP) accelerometers were installed at three positions on the third span, specifically on the damaged first girder from the north side and the middle girder. Fig. 13 shows a schematic view of the accelerometer and strain gauge locations on both girders. The vertical acceleration of the girders was recorded at six points under two
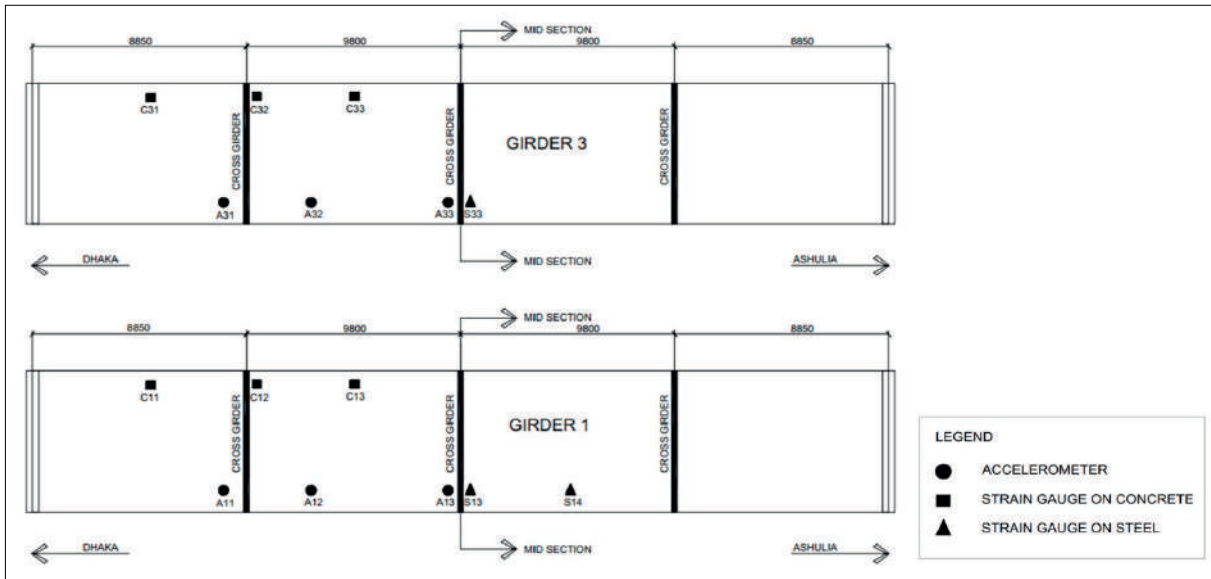
Fig. 13: Schematic view of the accelerometer position

different loading conditions. Fig. 14 shows how the accelerometers were attached to the girders for the test.

Fig. 14: ICP Accelerometers attached to the girders

The strain gauges used in these tests to measure concrete strain were models KFGS-5-120-C1-11-L3M2R and KFGS-30-120-C1-11-L5M2R, both manufactured by Kyowa Electronic

Instruments. These are general-purpose, single-axis strain gauges with lengths of 5 mm and 30 mm, respectively, and a resistance of 120 ohms. A picture of both strain gauges is shown in Fig. 15.

In this test, the vertical acceleration of specific points was measured on the girders under three loading conditions for both girders. The cases considered were:

• Ambient vibration
• A truck moving at a constant speed of 10 km/hour
• A 512 kg object dropped from a height of 5 feet

To study the dynamic effects on the damaged bridge span, a truck with a gross weight of 22,365 kg was used. During the dynamic loading tests, the truck moved at a constant speed of 10 km/hour across the span.

(a)   (b)

Fig. 15: Strain gauges attached to (a) Steel (b) Concrete

Fig. 16: Truck used for the test

Fig. 16 provides a side view of the truck used in the tests.

A heavy object weighing 512 kg was released from a height of 5 feet (9m from mid-point of the span on the 2nd girder) to perform the impact load test. Fig. 17 shows the object used for the impact load test.

Fig. 17: Heavy object being dropped for the impact load test

All the bridge response data for different loading conditions were recorded in a computer using a data logger for further analysis. Figures 18 to 23 show the frequency spectra of acceleration data at the midpoints of both girders under three different conditions. In all these frequency spectra a common peak is found around 3.43 Hz.
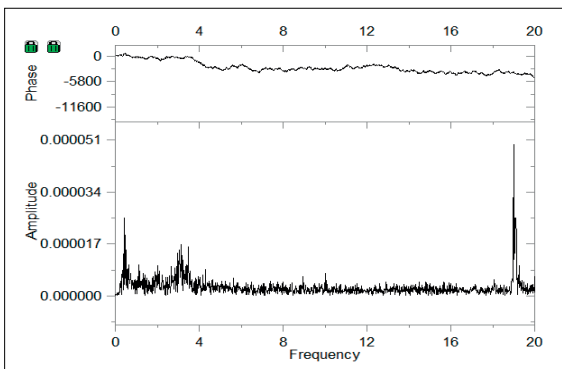
Fig. 18: Frequency spectrum of acceleration at the midpoint of the first girder (A13) under ambient conditions
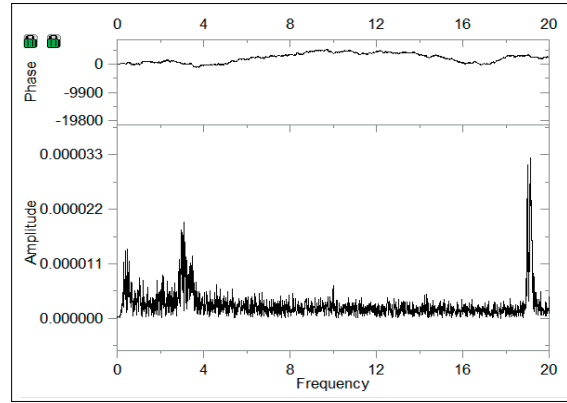
Fig. 19: Frequency spectrum of acceleration at the midpoint of the middle girder (A33) under ambient conditions
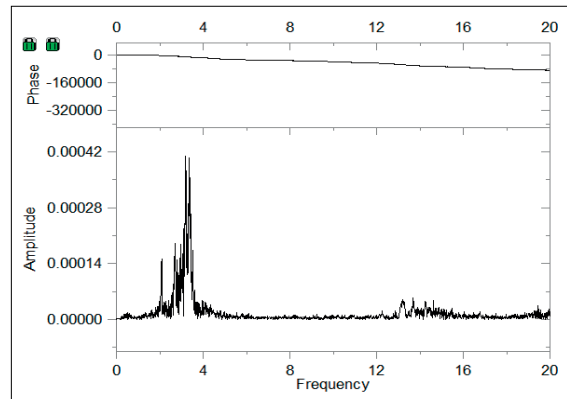
Fig. 20: Frequency spectrum of acceleration at the midpoint of the first girder (A13) under dynamic conditions
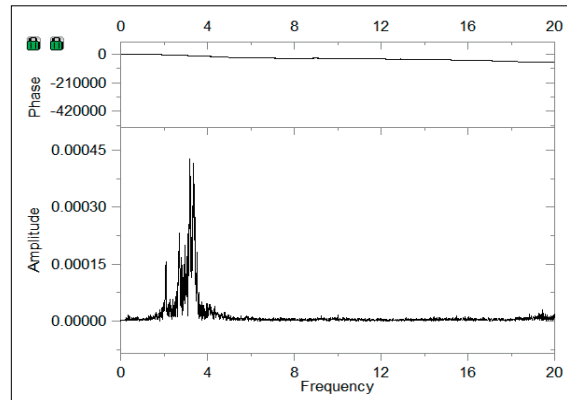

Fig. 21: Frequency spectrum of acceleration at the midpoint of the middle girder (A33) under dynamic conditions
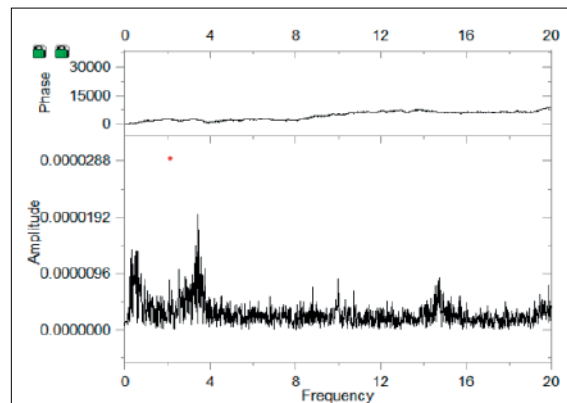

Fig. 22: Frequency spectrum of acceleration at the midpoint of the first girder (A13) under impact loading
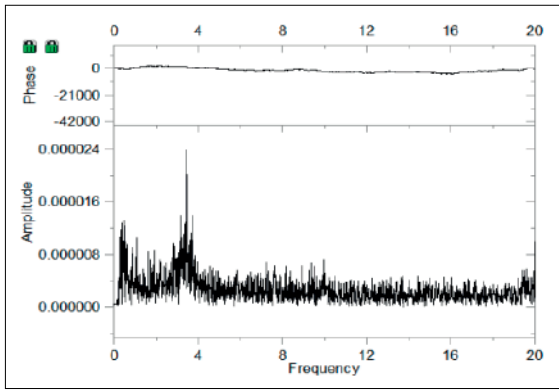
Fig. 23: Frequency spectrum of acceleration at the midpoint of the middle girder (A33) under impact loading

FINITE ELEMENT ANALYSIS

To validate the experiment, an analysis was conducted using CSiBridge v26.0.0 and Midas Civil 2021 software packages. The bridge was modeled under three different conditions: free vibration, truckload, and impact load, in order to calibrate the model using the results of the field testing. A 20% effective pre-stress loss was assumed to account for the damage sustained. Fig. 24 shows a 3D view of the finite element model of the bridge.
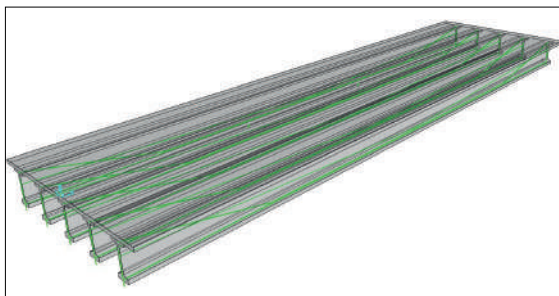

Fig. 24: Repaired bridge model on CSiBridge

RESULTS AND DISCUSSION

ACCELEROMETER DATA ANALYSIS IN THE FREQUENCY DOMAIN

The sample frequency of the data taken for the test was 1000 per second. Ambient vibration readings taken from the accelerometers were analyzed using Fast Fourier Transformation (FFT). FFT plots of data from different accelerometers of each girder are superposed to determine the dominant frequencies of the structure. Combined accelerometer responses in the ambient condition are shown in Fig. 25. Fig. 26 shows the frequency response of free vibration after impact loading. In the ambient condition, various local modes of vibration can be activated. However, following an impact

load, the bridge primarily resonates with its fundamental natural frequency during free vibration.
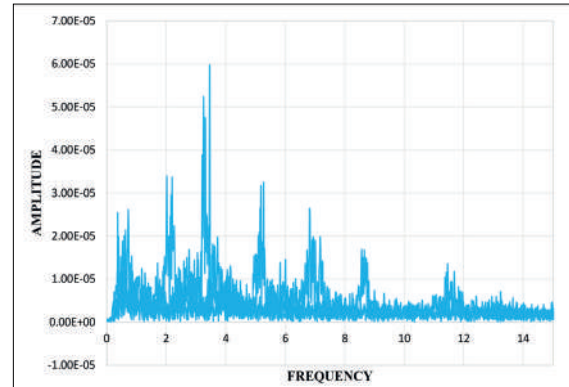

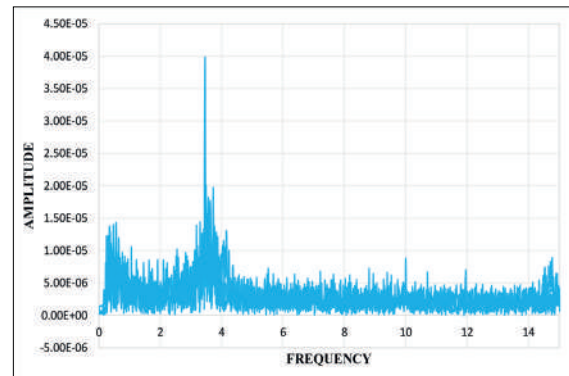Fig. 25: Ambient vibration response of both girders

Fig. 26: Free vibration response after impact

In both cases, the natural frequency was measured to be approximately 3.43 Hz. The CSiBridge and Midas Civil 2021 model also predicted a first mode frequency of 3.43 Hz, which validates the accuracy of the analysis.

STRAIN GAUGE DATA ANALYSIS

The maximum strain of concrete at different points on both the girders is shown in Tables 1 and 2. The energy input is much higher in the case of the impact load than in the truckload. Thus, the strain values are relatively higher for the impact load.

Table 1: Maximum concrete strain under the dynamic truck load	
Strain Gauge Serial	**Reading**
C11	0.000633
C12	0.001055
C13	0.003165
C31	Invalid
C32	0.000633
C33	0.000844

Table 2: Maximum concrete strain under the impact load	
Strain Gauge Serial	**Reading**
C11	0.001266
C12	0.001477
C13	0.003376
C31	Invalid
C32	0.004031
C33	0.000844

The finite element model of the bridge was calibrated by changing the modulus of elasticity and prestress to match the natural frequency and the maximum strain of concrete under the impact load. This analysis shows a maximum strain of 0.004 at a location 9 meters from the midpoint, which closely matches the strain measured by the strain gauge (C32) at the corresponding location.

BRIDGE LOAD RATING RESULTS

A time history analysis was initially performed on the bridge using the AASHTO standard HL-93K truck loading. The analysis revealed that stress limits were exceeded at critical sections of the bridge (Fig. 27). These results
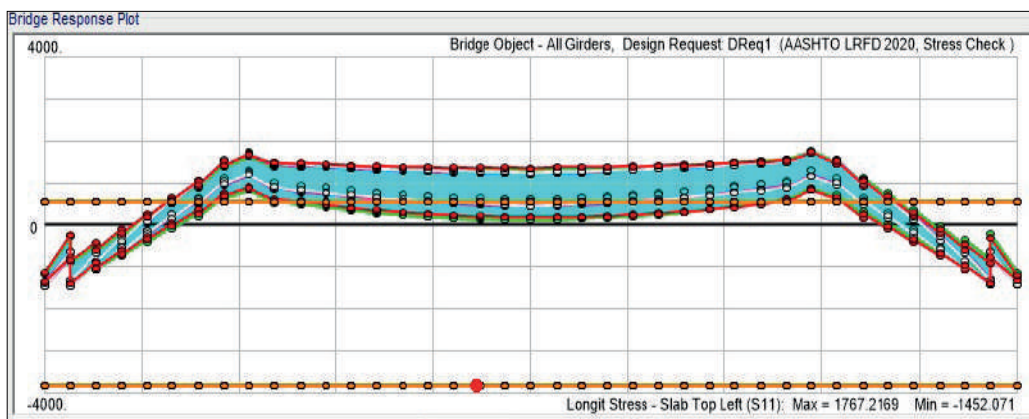

Fig. 27: Stress exceeds the limit at the left Girder for AASHTO standard truck (HL-93k truck)
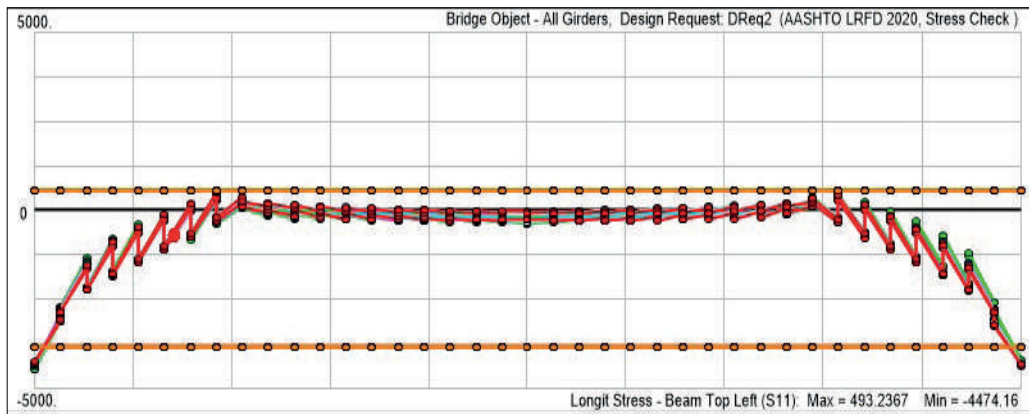

Fig. 28: Stress within the limit at the left Girder for 20-ton truck
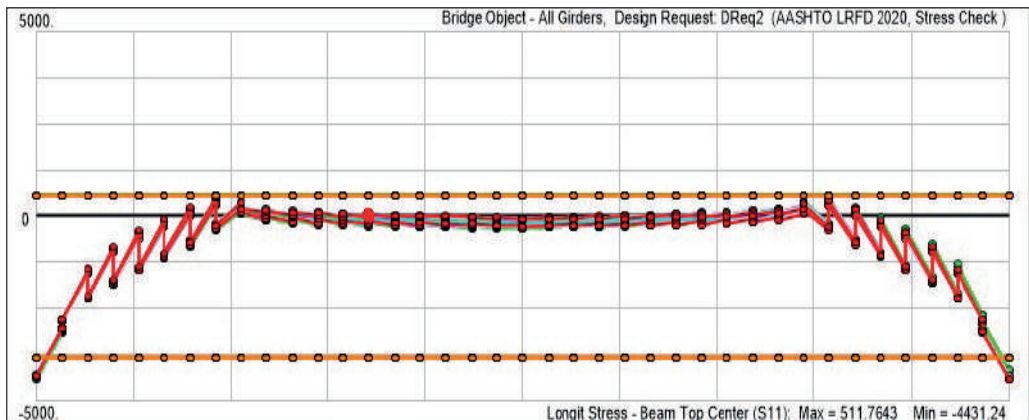

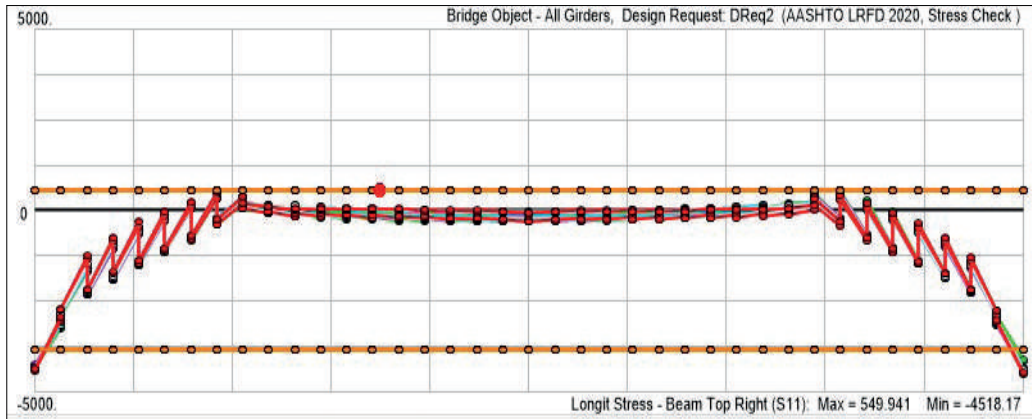Fig. 29: Stress within the limit at center Girder for 20-ton truck

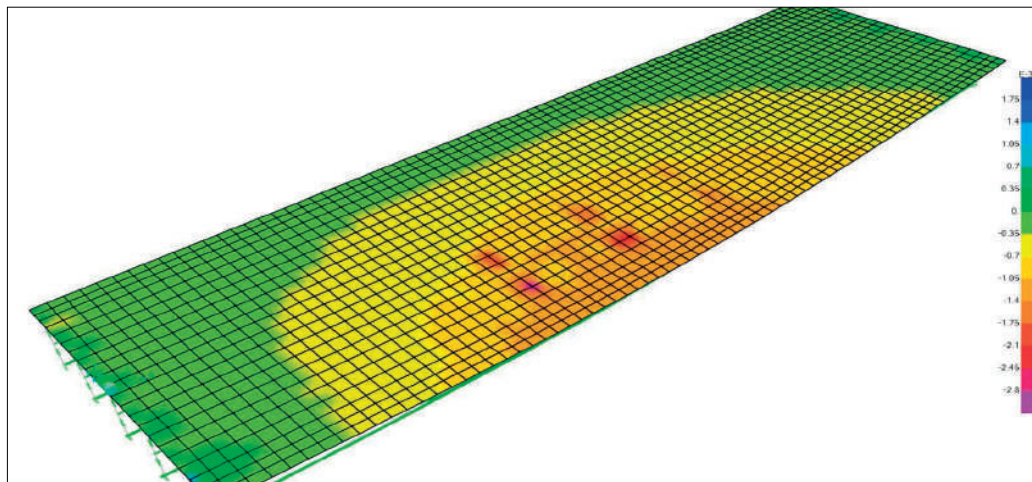Fig. 30: Stress within the limit at right Girder for 20-ton truck

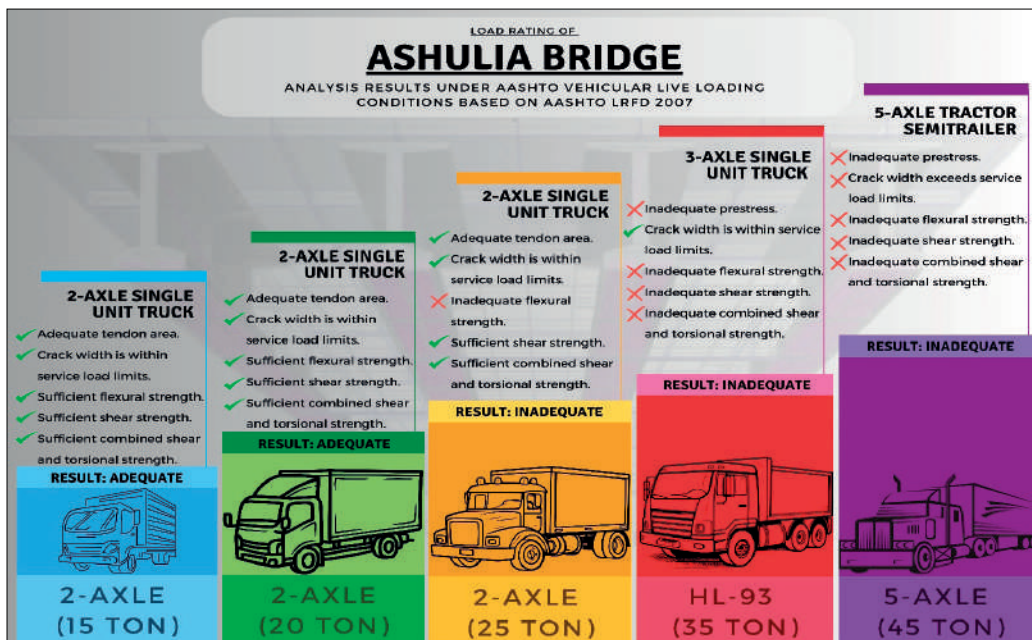Fig. 31: Stress distribution for 20-ton truck

Fig. 32: Load rating chart under different truck loading conditions for the Ashulia Bridge

suggest that the current design is insufficient to accommodate the expected loading conditions in Service I load combination, indicating the need to reduce truck weight to meet the required safety standards.

After conducting several trials, it is determined that a 20-ton truck meets the structural criteria of the bridge, ensuring that the stress limits are not exceeded at critical sections under dynamic loading conditions. Figures 27 to 30

illustrate that the right, left and center girders of the bridge remain within acceptable stress limits according to AASTHO 2020 guideline (Service II Load Combination). Fig. 31 displays the stress distribution on the deck of the bridge under the dynamic load of a 20-ton moving truck in Service II load combination. Based on the findings of this study, a load rating chart Fig. 32 was produced for communication among the stakeholders.

CONCLUSIONS

This study presents an assessment of the post-repair load-carrying capacity of the Ashulia Bridge, which underwent significant structural rehabilitation following damage caused by a collision. Experimental tests, including truckload and impact load assessments, were complemented by finite element analysis to evaluate the structural performance under various loading conditions.

The retrofitting measures, including crack repairs, spalling restorations, and CFRP strengthening, effectively restored the structural integrity of the damaged girders. These repairs are critical for ensuring the bridge's continued operation during the interim period before the elevated expressway becomes operational.

A calibrated finite element model developed using CSiBridge and Midas Civil software accurately predicted the bridge's natural frequency and strain responses. These predictions closely matched the results obtained from field experiments, reinforcing the model's reliability. The bridge was determined to safely accommodate a maximum vehicular load of 20 tons.

The experimental and analytical methodologies employed in this study can serve as a reference for similar assessments of precast-prestressed I-girder bridges subjected to damage. The integration of field testing with numerical modeling provides a comprehensive framework for evaluating structural adequacy.

REFERENCES

1. American Association of State Highway and Transportation Officials. The Manual for Bridge Evaluation. 3rd edition, American Association of State Highway and Transportation Officials, 2018.

2. Polepally, G., Neridu, S., Pasupuleti, V. D. K., & Kalapatapu, P. (2024). Experimental and Numerical Investigation of Axial Load Capacity for Box-type Railway Bridges. In Procedia Structural Integrity (Vol. 52, pp. 487–505). Elsevier BV. https://doi.org/10.1016/j.prostr.2023.12.049.

3. Ataei, S., Aghakouchak, A., Marefat, M., & Mohammadzadeh, S. (2005). Sensor fusion of a railway bridge load test using neural networks. In Expert Systems with Applications (Vol. 29, Issue 3, pp. 678–683). Elsevier BV. https://doi.org/10.1016/j.eswa.2005.04.038.

4. Naser, A. F., Mohammed, H. A., & Mohammed, A. A. (2022). Flexure and shear load rating evaluation of composite bridge superstructure under effect of different trucks load types. In Materials Today: Proceedings (Vol. 57, pp. 398–407). Elsevier BV. https://doi.org/10.1016/j.matpr.2021.12.268.

5. Saroufim, A., Issa, M. A., Mahdi, M., & Issa, M. A. (2023). Proof load testing and shear assessment of kishwaukee I-39-river bridge using the modified compression field theory. In Journal of Civil Structural Health Monitoring (Vol. 13, Issues 2–3, pp. 827–866). Springer Science and Business Media LLC. https://doi.org/10.1007/s13349-022-00667-0

6. Bridge Maintenance System (BMMS), Roads and Highway Department, People Republic of Bangladesh. https://www.rhd.gov.bd/BridgeDatabase/BCS3.asp?vStructureID=120316&vRoadID=21&vSurveyYear=2013&vSubdivID=510.

7. Shukla, A. K., Maiti, P. R., & Rai, G. (2020). Retrofitting of Damage Rail Bridge Girder and Its Performance Evaluation. In Journal of Failure Analysis and Prevention (Vol. 20, Issue 3, pp. 895–911). Springer Science and Business Media LLC. https://doi.org/10.1007/s11668-020-00890-1.

8. Srivastava, S., & Mishra, A. (2024). Flexural and shear load rate evaluation on Pre-stressed concrete Box Girder Superstructure under the effect of IRC Loading. In IOP Conference Series: Earth and Environmental Science (Vol. 1326, Issue 1, p. 012004). IOP Publishing. https://doi.org/10.1088/1755-1315/1326/1/012004.

9. Mirdad, M. A. H., & Andrawes, B. (2023). Experimental and analytical approaches for load rating reinforced concrete slab bridge. In Advances in Structural Engineering (Vol. 26, Issue 13, pp. 2447–2464). SAGE Publications. https://doi.org/10.1177/13694332231188417.

10. Navrátil, J., Drahorád, M., & Ševčík, P. (2017). Assessment of Load-Bearing Capacity of Bridges. In Solid State Phenomena (Vol. 259, pp. 113–118). Trans Tech Publications, Ltd. https://doi.org/10.4028/www.scientific.net/ssp.259.113.

11. Alampalli, S., Frangopol, D. M., Grimson, J., Halling, M. W., Kosnik, D. E., Lantsoght, E. O. L., Yang, D., & Zhou, Y. E. (2021). Bridge Load Testing: State-of-the-Practice. In Journal of Bridge Engineering (Vol. 26, Issue 3). American Society of Civil Engineers (ASCE). https://doi.org/10.1061/(asce)be.1943-5592.0001678.

12. Omar, T., & Nehdi, M. L. (2018). Condition Assessment of Reinforced Concrete Bridges: Current Practice and Research Challenges. In Infrastructures (Vol. 3, Issue 3, p. 36). MDPI AG. https://doi.org/10.3390/infrastructures3030036.

WORKSHOP ON
BUILDING RESILIENT INFRASTRUCTURE FOCUS ON EARTHQUAKE & FIRE SAFETY

The Department of Civil Engineering at **Manipal Institute of Technology**, in association with **Seismic Academy** (an Initiative by **HILTI**) organized a workshop on October 4, 2024, focusing on resilient infrastructure design and disaster preparedness.

The inaugural Session was presided by Cdr. (Dr.) Anil Rana, Director, Manipal Institute of Technology and Dr. Purushotham G. Sarvade, Head Civil Engineering Department, Manipal Institute of Technology.

The technical sessions were delivered by Dr. Rupen Goswami (Professor, IIT Madras), Dr. Palanisamy (Professor, NIT Surathkal) and Mr. Shounak Mitra (Head Codes and Approval, Fastening, Hilti India Pvt Ltd) focusing on the aspect of earthquake-resistant design of structures.

Mr. Leslie Joseph Dsouza (Chief Fire Officer, Manipal Academy of Higher Education) and Mr. Raghavendra Kumar V (Head Codes and Approval Fire Protection) deliberated on the topic of fire safety in buildings.

Dr. Amarnath CB (India BIM Association) highlighted on the applications of digital trends in construction industry.

The workshop, convened by Mr. Laxman Kudva P. and Dr. H. K. Sugandhini, concluded with an emphasis on advanced materials, fire safety and digital innovation for resilient infrastructure.

TEXTILE FIBRES REINFORCE A BUILDING - KOMATSU SEIREN

With the four main islands of Japan perched atop a convergence of three major tectonic plate boundaries, the country has a history of strong earthquakes from time to time. The impact of repeated seismic activities on buildings, infrastructure and population is significant and calls for some of the finest and advanced engineering designs for the buildings.

With standard rigid frame construction, whether steel or reinforced concrete framing, a typical seismic reinforcement strategy is to add stiffening elements, such as cross bracing, within the centre core of a building and at key structural corners. Also, energy dissipating devices like seismic dampers and isolators are used to protect the building during major earthquake shifts. However, innovation in engineering has attained a new height with the use of an extremely unconventional yet effective

technology in Japan. A Japanese textile firm, Komatsu Seiren, used high-tensile strand rod developed from thermoplastic carbon fibre composite as seismic reinforcement to strengthen its facility in Nomi, Japan. Architects Kengo Kuma and Associates attached more than 1,000 of these high-tensile rods to the roof of the facility. Inside the showroom, another "curtain" of nearly 3,000 additional rods added further structural reinforcement. Together these systems helped minimize the horizontal forces exerted during an earthquake. Drawing from a technique of braiding ropes in this region, it became possible to add further flexibility to the carbon fibre. The project presents a tasselled view focusing on specific materiality with the new facade design.

The Factory Laboratory project utilized the strand rod that Komatsu Seiren was developing,

which is a thermoplastic carbon fibre (CF) composite that was tested to be seven times stronger than an equivalent diameter iron rod but is much lighter in weight.

The composite assembly (or CF rod) has high tensile strength with exceptional flexibility and lightness and the project marks it as the world's first structure in which a CF composite strand is used for seismic reinforcement.

Technically, fibres are strong in tension, and this was what Kuma did by "draping" the thermoplastic CF composite rods (or cables) on the exterior of the building. The strands were secured at the top. The bottom ends of the strands were anchored in the ground outside the main floor on three sides of the building. Rather than simply pulling the cables taut in an even curving arc around the base of the building, Kuma has added interest to the draping by undulating the edge and holding sections of the strands apart at ground level to create open access to the building entrance.

The building used both internal cross-bracing (utilizing CF rod assemblies) and exterior-draped fibres to achieve the stabilization needed. The internal cross-bracing locations were the partition brace-bearing walls strategically located to reinforce the existing building frame. The CF rods were arranged in a diagonal mesh pattern set within rectangular floor-to-ceiling-high steel frames that fit within and were fastened to the building's existing structural frame. The two systems have to work together in order to dampen any seismic impact on the structural frame; without the internal brace-bearing walls, the exterior cable bracing would cause the building's structural frame to compress, risking collapse or compression of the floors in the event of an earthquake.

REFERENCES

1. The Most Earthquake-Resistant Structures on Earth | Digital Trends

2. Kengo Kuma Uses Carbon Fiber Strands to Protect Building from Earthquakes | ArchDaily

3. Textile fibers reinforce a building - Fabric Architecture Magazine

4. Kengo Kuma uses new carbon fibre composite to reinforce buildings against quakes | Architecture & Design

5. Komatsu Matere Offices, Nomi - Kengo Kuma | Arquitectura Viva

THE GREAT SUMATRA EARTHQUAKE – 20 YEARS INTO THE DEVASTATION

It has been twenty years since we witnessed the mega Sumatra-Andaman Earthquake, one of the most devastating seismic events in the last forty years. People woke up on a fine December morning (26 December 2004) only to be witness to the deadly tsunami wreck the coastal areas of a dozen countries in South and South-east Asia. Infact, this happened to record the third highest number of death toll by any earthquake since 1960, after the 2010 Haiti earthquake and 1976 Tangshan earthquake.
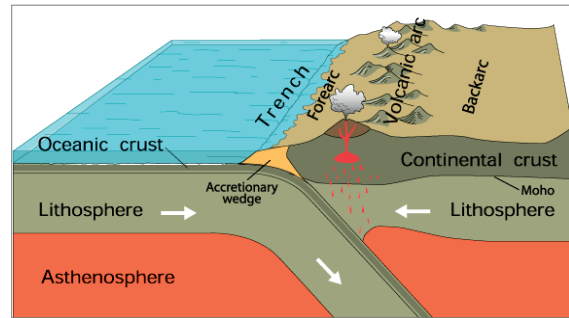

Fig. 2: General diagram of an oceanic subduction zone
(Source - Tsunami Generation from the 2004 M=9.1 Sumatra-An-daman Earthquake | U.S. Geological Survey (usgs.gov))
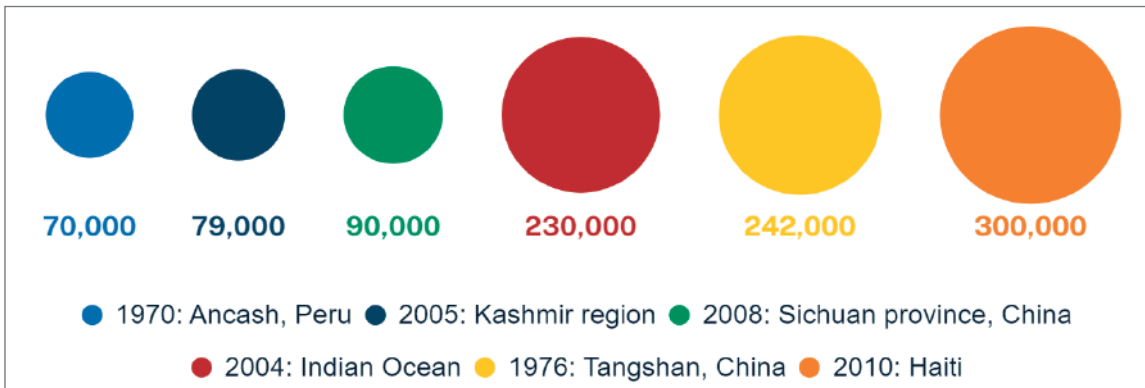

Fig. 1: Most Destructive Earthquakes Since 1960 With Highest Death Toll
(Source - Notable Earthquakes in History | Major Earthquakes, Destruction & Aftermath | Britannica)

An undersea earthquake with a magnitude of 9.1 struck off the coast of the Indonesian island of Sumatra at around 7 am in the morning. Over the next seven hours, a tsunami (a series of immense ocean waves) triggered by the quake reached out across the Indian Ocean, devastating coastal areas. Some locations reported that the waves had reached a height of 9 metres or more when they hit the shoreline.

It occurred along a tectonic subduction zone in which the India Plate, an oceanic plate, was being subducted beneath the Burma micro-plate which was part of the larger Sunda plate. The interface between the two plates resulted in a large fault, termed an inter-plate thrust or megathrust. The direction of convergence of the India Plate relative to the Sunda plate was oriented oblique to the orientation of the inter-plate thrust (i.e., trench axis). For oblique subduction zones such as this, movement between the two plates can be accommodated in one of two ways as shown in the block diagram (Michael, 1990) (refer Fig 3). As described in a classic paper by Fitch (1972), the Sumatra subduction zone is characterized by decoupled faulting (refer Fig. 3b). In this
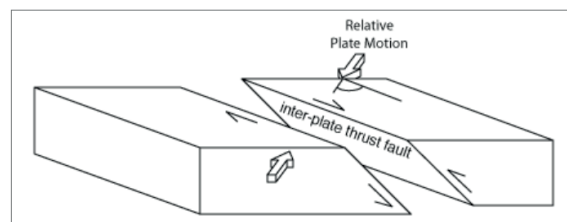
3a. Oblique thrust faulting
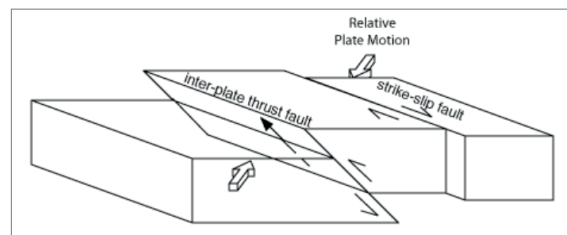
3b. Decoupled faulting

Fig. 3: Types of faults
(Source - Tsunami Generation from the 2004 M=9.1 Suma-tra-Andaman Earthquake | U.S. Geological Survey (usgs.gov))

case, nearly pure thrust faulting occurs along the inter-plate thrust and strike-slip faulting occurs in the overriding plate, most notably along the Great Sumatran fault.

The tsunami from the Sumatra-Andaman earthquake was primarily caused by vertical displacement of the seafloor, in response to the slip on the inter-plate thrust fault. The seafloor on the overriding Burma plate deformed vertically, uplifting seaward toward the trench and subsiding landward toward the coastline. Vertical displacement of the water column approximated that of the seafloor below, resulting in the initial "N-shaped" tsunami wave that was typically generated by subduction earthquakes. This N-wave then split into two, resulting in a pair of N-waves traveling in opposite directions – the distant tsunami, propagated outbound across the Bay of Bengal towards India and Sri Lanka, eventually reaching the Atlantic and Pacific Oceans and the local tsunami, travelled towards Indonesia, Thailand, and nearby islands in less than an hour. The length of the fault that ruptured during this earthquake was massive, extending from northwest Sumatra north to the Andaman Islands.
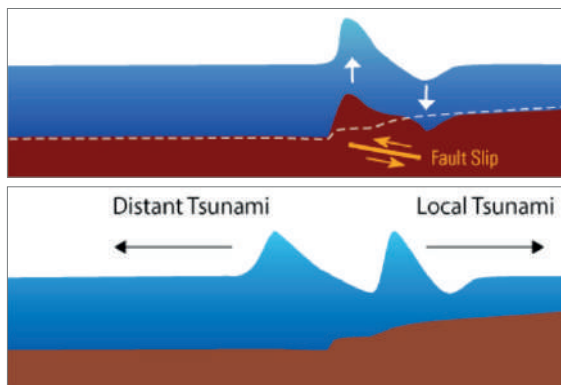

Fig. 4: Schematic diagram of tsunami generation and splitting
(Source - Tsunami Generation from the 2004 M=9.1 Sumatra-Anda-man Earthquake | U.S. Geological Survey (usgs.gov))
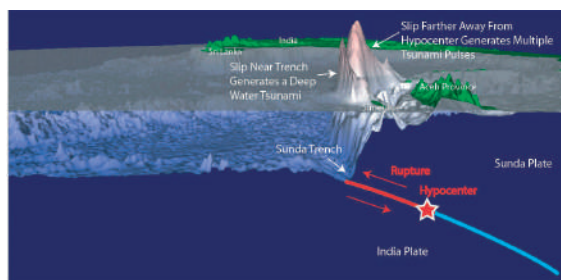

Fig. 5: Sumatra Earthquake Occurrence
(Source - Tsunami Generation from the 2004 M=9.1 Suma-tra-Andaman Earthquake | U.S. Geological Survey (usgs.gov))

The earthquake was strongly felt in northern Sumatra and in the Indian Andaman & Nicobar Islands i.e. along the rupture. The strongest shaking was experienced on the island of Simuelue off the coast of Sumatra. In Sumatra, strong tremors were experienced along the west coast at places such as Kembang Cot and Meulaboh that caused number of buildings to collapse. Further inland, landslides were triggered in the Barisan Mountains and some buildings were damaged at Takaptuan. In the larger cities of Medan and Banda Aceh the shaking had varied effects. In Medan, although the quake was frightening enough to send people running outdoors and to cracks some windows, the city fared much better than Banda Aceh where some newer modern high-rise suffered extensive damage. Damage to buildings was also reported from the Andaman & Nicobar Islands. In the Nicobar Islands, buildings were damaged on the islands of Car Nicobar, Katchall and Nancowry. At Campbell Bay on Great Nicobar Island though many of the low-rise buildings escaped with hairline cracks some newer buildings suffered non-structural damage. Liquefaction was observed on Car Nicobar Island. In the Andaman Islands, damage was similar as in Indonesia, with newer buildings suffering more damage as compared to older & low-rise structures. In Port Blair, the earthquake began as a noticeable tremor that progressed into a strong shaking that made it difficult to remain standing. Farther away, to the east the quake was felt in many parts of Malaysia, Singapore and Thailand. he tremor was also felt in Bangkok, Chiang Mai and other cities in Thailand. Several high-rise buildings were evacuated in Malaysia, including at Pinang and Port Klang. The shock was also felt at Alor Star and Pangkor. Residents of Singapore also felt the earthquake. To the west, the quake was felt at several locations in peninsula India as well as in the Bengal. Minor damage was reported form Barisal, Chandpur Sadar, Chittagong as well as Dhaka in Bangladesh. In India, the quake was distinctly felt along the east coast. In Tamil Nadu, people felt distinct tremors in most parts of Chennai as well as at Pondicherry & Tuticorin. It was also felt at Bhubaneswar and in towns in the Mahanadi delta, Mayurbhanj,

Jajpur, Koraput and Sunabeda. Tremors were also reported from the coastal belt of Andhra Pradesh from Srikakulam to Chittoor as well as in the cities of Nellore, Vishakhapatnam and Vizianagaram. Severe shaking was also felt in Kochi and Bengaluru. In West Bengal, the quake was also felt in Kolkata. Tremors were also felt at Dhanbad and the surrounding towns in Jharkhand. Many places in Sri Lanka, such as Kandy also felt the tremors for a prolonged period.

Several powerful aftershocks were reported from the region. Additional strong earthquakes were reported from the adjoining parts of the Andaman & Nicobar Islands within hours of this earthquake. Many of these earthquakes occurred in or near the main islands in this archipelago. 23 aftershocks with magnitude in excess of 6.0 were recorded over the next few weeks. These aftershocks clearly delineated a 1,000+ kilometre section of the plate boundary between the Indian Plate and the Burmese Micro-Plate that ruptured in the mainshock. Some of the larger aftershocks were strong enough to be felt as far as Chennai on the east coast of India.

The earthquake also caused energetic seismic seiches in water bodies in Assam, Jharkhand, Maharashtra, Manipur, Orissa and West Bengal. Seismic seiches were seen in other parts of Kolkata as well as in Bhubaneswar, Balasore, Puri in Orissa. Similar phenomena were also observed in Dhanbad and Rajganj. Eruptions of natural gas that ignited along with eruptions of mud volcanoes were reported from locations along Burma's Arakan coast and also in Sandoway. In Middle Andaman Islands, at Baratang, an older mud volcano became active again after the earthquake (refer Fig. 6) and also several new small mud volcanoes erupted which severely affected the sea traffic and hence the relief operations.

Fig. 6: Eruption of a mud volcano near Jarawa Creek at Baratang Island in Middle Andaman
(Source - FEB10C1.PDF (iitk.ac.in))

A team of experts consisting of Dr. Sudhir K. Jain, Dr. C. V. R. Murty, Dr. Durgesh C. Rai, Dr. Javed N. Malik, Ms. Alpa R. Sheth, Mr. Arvind Jaiswal, Dr. Snigdha A. Sanyal, together with few undergraduate students carried out a detailed investigation and furnished their findings of the tsunami reconnaissance, a brief of which is captured in this write-up.

Aerial surveys were carried out along most of the Nicobar Islands and over Little, South, and Middle Andaman Islands as well as field investigations performed in the North, Middle, South, and Little Andaman Islands and the Car and Great Nicobar Islands indicated complex distribution of damage across these areas (refer Fig. 7).
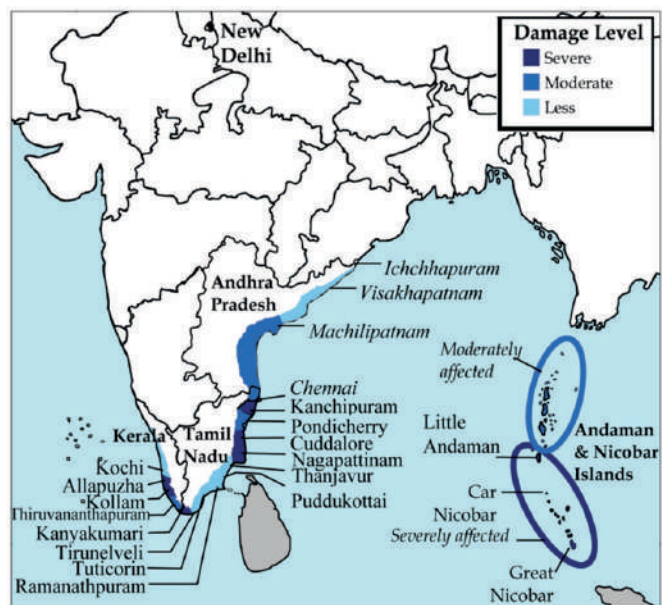

Fig. 7: Map showing relative tsunami-induced damage along the coastal districts and in the islands
(Source - April-05-Sumatra_FINAL4.indd (nicee.org))

According to one of the records, 2,30,210 people were estimated to have been killed in the Indian Ocean-wide tsunami generated by this earthquake - 1,84,168 of these were confirmed and 45,752 were missing. The highest death toll was from Sumatra where 1,30,736 persons were confirmed dead. This was followed by Sri Lanka where 35,322 fatalities were confirmed. 12,504 deaths were recorded in India.

According to another official statistic (www.ndmindia.nic.in 2005), the total number of Indian fatalities were 10,805, with over 5,640 persons missing. The state of Tamil Nadu had the highest number of fatalities — 8,010

(www.tn.gov.in/tsunami 2005) - with the district of Nagapattinam alone accounting for 6,065 deaths. However, as a percentage of the total population, the statistics from the Nicobar Islands indicated the most severe losses – out of the total population of 42,068, about 1,395 were reported dead and 5,764 were missing. Most of the tsunami victims on the mainland belonged to the fishing community or lived in houses within 500 m of the water. Tourists in Velankanni in the state of Tamil Nadu and morning walkers in urban areas (Karaikal, Chennai and Pondicherry) were also succumbed to this natural disaster.

While damage in Little Andaman Island and all Nicobar Islands was predominantly tsunami-related, that in the islands north of Little Andaman was primarily due to earthquake shaking, though tsunami waves and high tides were also an issue. In general, the building stock consisted of a large number of traditional and non-engineered structures. Many traditional structures were made of wood, and they performed well in the earthquake shaking (refer Fig. 8). However, a number of new, poorly constructed reinforced concrete (RC) structures suffered severe damage or even collapse due to shaking (refer Fig. 9).

Fig. 8: Single-story wood house in Port Blair with light roof had no damage
(Source - April-05-Sumatra_FINAL4.indd (nicee.org))

Fig. 9 Three storied RC framed building collapsed
(Source - April-05-Sumatra_FINAL4.indd (nicee.org))

The tsunami waves caused severe destruction in the coastal areas of the southern islands (refer Fig. 10). Structures near the water were subjected to a positive water pressure when the waves arrived, and a suction pressure when the waves receded. A large number of buildings right on the water in Little Andaman and Car Nicobar Islands were washed away, regardless of how they were constructed. However, an occasional well-designed RC structure was seen standing even in the devastated areas. In the best of the cases, the frame of the infilled building was intact, while the infills were pushed out of plane. In some cases, where there were a number of buildings in a row normal to the shore, the waves destroyed the structures towards the shore, but buildings in the rear were shielded. However, the number of buildings that survived is a very small fraction of the total houses near the shore.

Fig. 10: General destruction of built environment
(Source - April-05-Sumatra_FINAL4.indd (nicee.org))

In the northern Andaman and Nicobar Islands, tsunami-induced damage to the contents of buildings was significant, but there was less damage to the structure of buildings. For instance, in the Bamboo Flat area, the street front shops were inundated by the tsunami and the subsidence of land. The steel shutters of the shops were damaged. In some other buildings in the same region, the boundary walls collapsed.

In some of the masonry houses with load-bearing walls and light roof trusses made of either steel pipes or timber, the walls were not tied together to create lateral resistance. As a result, large movement of the flexible roofs from earthquake forces caused out-of-plane masonry wall to collapse. Similar damage

was observed at a much larger scale in many school buildings, where the long partition walls separating two classrooms were either badly damaged or had fallen due to out-of-plane instability (refer Fig. 11).

Fig. 11: Slender masonry walls dislodged due to out-of-plane instability
(Source - April-05-Sumatra_FINAL4.indd (nicee.org))

In general, RC frame structures suffered a variety of damage due to earthquake shaking, from frame infill separations and hinging at the ends of frame members, to collapse of structures. Despite the fact that ductile detailing has been mandated by the code for high seismic zone, not all buildings were properly designed and built to ensure ductile response. Generic RC structures were built in the Andaman and Nicobar Islands for community facilities and for government office buildings. These structures were severely damaged during the shaking. Some of the structures sustained severe cracking to its infill walls and its brittle RC columns in the open ground storey (refer Fig. 12).

Almost all the housing in the affected areas was non-engineered. Much of it was made of plastered masonry walls (usually brick) and sometimes of reeds, with roofs either of thatch, Mangalore tiles, or reinforced concrete. A large number of traditional structures built within 500 m of the water were destroyed. Along the Kerala coast, the damage and collapses of the housing stock appeared to be largely due to the scouring action of the waves, primarily the receding ones.

A newly constructed 268 m-long RC bridge over the Austen Strait, connecting the North and Middle Andaman Islands on the Andaman Trunk Road, had to be closed to even light vehicles. Three middle spans of the superstructure were displaced laterally by about 70 cm and vertically by about 22 cm and fell off the bearing (refer Fig. 13). Some other spans were also moved laterally by about 2 cm to 15 cm.

Fig. 12: Building showing severe cracking and damage to soft ground storey
(Source - April-05-Sumatra_FINAL4.indd (nicee.org))

Fig. 13: Bridge over Austen Strait was rendered dysfunctional
(Source - April-05-Sumatra_FINAL4.indd (nicee.org))

Along the Tamil Nadu coast, there was significant damage due to the direct pressure of the water waves; however, no instances of fatalities in collapsed structures were noted. Bridges and culverts were affected. At least

Fig. 14: Loss of spans of the four span RC bridge at Melmannakudi in Tamil Nadu
(Source - April-05-Sumatra_FINAL4.indd (nicee.org))

three bridges were damaged, with one of them losing all four spans (refer Fig. 14).

The Car Nicobar runway was damaged at the junctions of the panels during the ground shaking. The damage was accentuated by the numerous landings made by the large transport aircraft bringing relief in the aftermath of the disaster. When spalling of the plain concrete was noticed at the junctions, landings of the large aircraft had to be discontinued and repairs were made. An 80 m segment of the approach jetty in Campbell Bay in Great Nicobar Island collapsed, thereby hampering relief efforts. Similarly, the collapsed jetty in Car Nicobar Island, and the breaching of one breakwater-cum-approach jetty and collapse of another approach jetty in Little Andaman Island also hampered relief efforts. In Port Blair, the Janglighat jetty collapsed. In the North Andaman Islands, jetties at Sagardeep and Arial Bay were damaged due to ground shaking. Pounding damage at several sections of jetties was observed.

The main source of electric power was from captive diesel-generator power plants. The 20 MW Suryachakra power plant in Port Blair was adversely affected by the tsunami waves, which flooded the entire plant. Severe damage to the equipment caused the plant to cease its operations temporarily. On Car Nicobar Island, power generation was disrupted by both flooding of the generators with saline water and displacement of generators by the tsunami waves.

Longitudinal cracks developed at the crest of the 27 meter high, 146 meter long rock-fill dam of the 5.25 MW Kalpong hydro-electric project near Diglipur in North Andaman Island. The cracks developed near the curved end along the axis of the straight portion of the dam.

Misalignment of turbines caused disruption of electric generation. Other facilities like hospitals and seaport/airport control towers collapsed due to shaking and/or wave pressure. The airport control tower at Car Nicobar was a three-story RC frame with masonry infills, and its upper story collapsed due to the shaking (refer Fig. 15). The seaport control tower at Hut Bay on the east coast of Little Andaman Island also collapsed due to the tsunami waves (refer Fig. 16).

Fig. 15: Partial-collapse of the upper story of the air traffic control tower at airport
(Source - April-05-Sumatra_FINAL4.indd (nicee.org))

Fig. 16: Laterally toppled three-story seaport traffic control tower at Hut Bay
(Source - April-05-Sumatra_FINAL4.indd (nicee.org))

While the 2004 earthquake left a permanent mark on the mind of people and some of the inhabitants of the affected areas are still recovering from the aftermath, the landmass has been shaken time and again over the past years. A total of 479 earthquakes with a magnitude of four or above have struck within 300 km of Andaman and Nicobar Islands

in the past 10 years. This comes down to a yearly average of 47 earthquakes per year. On average an earthquake will hit near Andaman and Nicobar roughly every 7 days. A relatively large number of earthquakes occurred near Andaman and Nicobar Islands in 2022 where the tremors (magnitude 4+) were detected more than 100 times within 300 km of Andaman and Nicobar that year. The strongest one was a 5.4 magnitude. Over the last three years, approximately 25 earthquakes of magnitude 5.0 or more have been recorded, the latest being a 5.2 magnitude on 19th September 2024 (183 km from Port Blair).

To conclude the earthquake and tsunami of 26 December 2004 highlighted the vulnerability of civil infrastructure and population inhabiting the Indian territories which are well known to have significant seismic hazard. The lack of adequate preparedness against the probable ground shaking by way of not designing the structures for earthquake resistance, led to failure of many buildings and structures when they were needed most for the rescue and relief operation. Further, the hazard posed by tsunami to Indian coastal regions which has been conveniently ignored thus far, should become one of the major considerations while developing civil infrastructure in these areas. The Indian standards for earthquake resistant design of structures are being developed and improved to safeguard a structure against any failure – it requires proper adoption and implementation at all levels. This will help to create a disaster resilient built environment and make construction better.

REFERENCE

1. Sumatra, Indonesia Earthquake and Tsunami, 26 December 2004 | NCEI (noaa.gov)

2. FEB10C1.PDF (iitk.ac.in)

3. April-05-Sumatra_FINAL4.indd (nicee.org)

4. Effects of M 9 Sumatra earthquake and tsunami of 26 December 2004 (researchgate.net)

5. Indian Ocean tsunami of 2004 | Facts & Death Toll | Britannica

6. Tsunami Generation from the 2004 M=9.1 Sumatra-Andaman Earthquake | U.S. Geological Survey (usgs.gov)

7. Indian Ocean tsunami of 2004 | Facts & Death Toll | Britannica

8. Impact of Great December 26, 2004 Sumatra Earthquake and Tsunami on Structures in Port Blair | Journal of Performance of Constructed Facilities | Vol 21, No 2 (ascelibrary.org)

9. :: ASC :: 26 December 2004, M9.1 "Boxing Day" Earthquake & Tsunami/Sumatra-Andaman Earthquake/Indian Ocean Tsunami (asc-india.org)

10. NAE Website - Effects of the 2004 Sumatra-Andaman Earthquake and Indian Ocean Tsunami in Aceh Province

11. Modified_Andaman_Report.pdf (seismo.gov.in)

12. The complete Andaman and Nicobar, India earthquake report (up-to-date 2024). (earthquakelist.org)

SEISMIC ACADEMY

"Building to withstand earthquakes is not a cost - it's an investment in safety and survival."

FOR MORE DETAILS ON THIS INITIATIVE, PLEASE VISIT OUR WEBSITE

https://theseismicacademy.com